

See discussions, stats, and author profiles for this publication at: <https://www.researchgate.net/publication/40756930>

Beneficial effects of PTP1B deficiency on brown adipocyte differentiation and protection against apoptosis induced by pro- and anti-inflammatory stimuli

ARTICLE *in* CELLULAR SIGNALLING · DECEMBER 2009

Impact Factor: 4.32 · DOI: 10.1016/j.cellsig.2009.11.019 · Source: PubMed

CITATIONS

22

READS

36

5 AUTHORS, INCLUDING:



Soledad Miranda

Universidad Autónoma de Madrid

6 PUBLICATIONS 89 CITATIONS

[SEE PROFILE](#)



Águeda González-Rodríguez

Instituto de Investigación Sanitaria La Prin...

53 PUBLICATIONS 587 CITATIONS

[SEE PROFILE](#)



Jesus Revuelta

Harvard Medical School

11 PUBLICATIONS 95 CITATIONS

[SEE PROFILE](#)

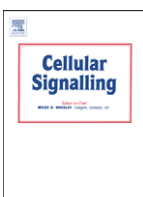


Angela Valverde

Institute for Biomedical Research “Alberto ...

77 PUBLICATIONS 1,301 CITATIONS

[SEE PROFILE](#)



Beneficial effects of PTP1B deficiency on brown adipocyte differentiation and protection against apoptosis induced by pro- and anti-inflammatory stimuli

Soledad Miranda ^{a,b}, Águeda González-Rodríguez ^{a,b}, Jesús Revuelta-Cervantes ^{a,b},
Cristina M. Rondinone ^{c,1}, Ángela M. Valverde ^{a,b,*}

^a Instituto de Investigaciones Biomédicas Alberto Sols (Centro Mixto CSIC/UAM), C/ Arturo Pérez Duperier 4, 28029 Madrid, Spain

^b Centro de Investigación Biomédica en Red de Diabetes y Enfermedades Metabólicas Asociadas (CIBERDEM), ISCIII, Spain

^c Metabolic Diseases Research, Global Pharmaceutical Research Division, Abbott Laboratories, Department 47R, Building AP10, 100 Abbott Park Road, IL 60064-6099, U.S.A.

ARTICLE INFO

Article history:

Received 29 October 2009

Received in revised form 18 November 2009

Accepted 28 November 2009

Available online 21 December 2009

Keywords:

PTP1B

Brown adipocytes

Apoptosis

TNF α

Resveratrol

ABSTRACT

Insulin is an inducer of brown fat adipogenesis through the activation of a signalling network that involves positive/negative modulators. Given the importance of brown adipose tissue (BAT) for basal thermogenic energy expenditure, we investigated the role of PTP1B in the acquisition of terminal differentiated phenotype and in the apoptotic responses of brown adipocytes. Immortalized brown preadipocytes lacking (PTP1B $^{-/-}$) or expressing (PTP1B $^{+/+}$) PTP1B have been generated. PTP1B deficiency accelerated a full program of brown adipogenesis including induction of transcription factors, coactivators, adipogenic markers and signalling molecules. Fully differentiated PTP1B $^{-/-}$ brown adipocytes were resistant to tumor necrosis factor (TNF α)-induced apoptosis as these cells were protected against caspase-8 activation, FLIP degradation, Bid cleavage and caspase-3 activation compared to wild-type controls. These events were recovered by PTP1B rescue. Survival signalling including phosphorylation of IRS-1 and Akt/PKB and BclXL expression were decreased in TNF α -treated PTP1B $^{-/-}$ cells but not in the wild-type. Similarly, PTP1B $^{-/-}$ brown adipocytes were protected against resveratrol-induced apoptosis. Phosphorylation of Akt/PKB and Foxo1 phosphorylation/acetylation decreased exclusively in resveratrol-treated wild-type cells, leading to nuclear localization of Foxo1 and up-regulation of Bim. Thus, PTP1B inhibition could be of benefit against obesity by counteracting TNF α -induced brown fat atrophy, and combined with resveratrol might improve low-grade inflammation.

© 2009 Elsevier Inc. All rights reserved.

1. Introduction

Brown adipose tissue is a major site for non-shivering thermogenesis in mammals. The unique thermogenic capacity of brown adipose tissue results from the expression of the uncoupling protein-1 (UCP-1) which uncouples fatty acid oxidation from ATP synthesis, allowing dissipation of energy from substrate oxidation as heat [1,2]. In addition, brown adipose tissue is a major site for lipid metabolism, and fatty acids are the main fuel to maintain the thermogenic capacity of the tissue (for a review, see [3]). Whereas it has been proposed that obesity in rodents is related to an impairment of adaptive thermogenesis possibly related to a functional atrophy of BAT [4], the relevance of BAT in adult humans has been a subject of controversy for

many years. However, a recent study has assessed the importance of BAT in adult humans and established a negative correlation between the amount of BAT deposition and the body-mass index [5].

It is well known that in rodents brown adipocytes differentiate at the end of the fetal life on the basis of two programs: an adipogenic program related to lipid synthesis and the expression of lipogenic enzymes, resulting in a multilocular fat droplet phenotype [6–8]; and a thermogenic program related to heat production and UCP-1 expression [9]. Despite a substantial knowledge of the molecular mechanisms of white adipogenesis, the understanding of the control of brown adipogenesis at the molecular level is still limited. With regard to adipogenesis, the C/EBP and PPAR families of transcription factors have an important role in the induction of the fully differentiated brown adipocyte phenotype. Regarding thermogenesis, C/EBP has been shown to transactivate the UCP-1 gene [10,11]. In fact, C/EBP expression increases in rat brown adipose tissue during late fetal development, concurrent with the expression of UCP-1 [7]. Moreover, the UCP-1 enhancer also contains a response element for PPAR γ [12]. The effect of PPAR γ is strongly increased by binding of the cold-inducible coactivator PGC-1 α (PPAR γ coactivator-1 α) through the ligand-dependent way [13,14]. Interestingly, both C/EBP and UCP-1 mRNAs are up-regulated by insulin in primary cultures of brown

Abbreviations: PBS, phosphate-buffered saline; FS, fetal bovine serum; BSA, albúmina bovina; T3, triiodo-thyronine; BAT, brown adipose tissue; TNF, tumor necrosis factor; IRS, insulin receptor substrate, PKB, protein kinase B; FLIP, FLICE inhibitory protein.

* Corresponding author. Instituto de Investigaciones Biomédicas Alberto Sols, C/ Arturo Pérez Duperier 4, 28029 Madrid, Spain. Tel.: +34 91 5854497; fax: +34 91 5854401.

E-mail address: avalverde@ib.uam.es (Á.M. Valverde).

¹ Present address: Metabolic Diseases, Hoffmann-la Roche Inc., 340 Kingsland Street, Nutley, New Jersey, 07110-1199, USA.

adipocytes. By contrast, PPAR γ expression in brown adipocytes seems to be insulin-independent [15]. PPAR γ and C/EBP α cooperatively regulate each other's expression and orchestrate a transcriptional cascade that maintains the stable differentiated state of the adipocyte [16–18]. However, ectopic expression of PPAR γ or C/EBP α in mesenchymal cells induces only a white, not a brown, fat phenotype, suggesting that these molecules do not control the determination of brown fat cell fate. Very recently, Tseng and co-workers [19] have demonstrated that bone morphogenetic protein 7 (BMP7) drives brown fat cell fate in both mesenchymal progenitor cells and committed brown preadipocytes, providing a novel target for anti-obesity therapies.

During the last years, the insulin receptor substrate (IRS) proteins have emerged as critical regulators of upstream signalling pathways leading to brown adipocyte differentiation. Substantial differences have been reported regarding the individual role of each family member. Whereas IRS-1 deficiency totally impairs brown adipocyte differentiation [20], the lack of IRS-2 allows brown fat cells to differentiate, although insulin-induced glucose uptake is impaired [21,22]. Moreover, both IRS-1 and IRS-3 are necessary for full UCP-1 expression in differentiated brown adipocytes [23] and for its induction in response to insulin in brown preadipocytes [15,24]. On the other hand, the protein tyrosine phosphatase 1B (PTP1B) is a negative modulator of insulin signalling by its ability to dephosphorylate the insulin receptor (IR) and IRS-1 in insulin target tissues [25,26]. The phenotype of PTP1B-deficient mice has revealed that the lack of this phosphatase confers protection against high fat diet-induced insulin resistance and obesity [27,28]. Accordingly, inhibition of this phosphatase has been proposed as a novel strategy for intervention in obesity and insulin resistant states. Although no differences in BAT mass were found in adult PTP1B $^{-/-}$ mice as compared to the wild-type controls, these mice exhibited increased energy expenditure [27,28]. However, the exact role of PTP1B in the regulation of brown adipogenesis remains to be determined.

Besides the beneficial effects of PTP1B inhibition on metabolism, other cellular responses such as cell adhesion, proliferation and programmed cell death are also regulated by this phosphatase [29]. In PTP1B $^{-/-}$ mice, activation of the death receptor (extrinsic) pathway in the liver upon injection of Jo2 is attenuated as compared with the profound apoptosis detected in wild-type mice [30]. Moreover, PTP1B $^{-/-}$ -deficient hepatocytes are protected against apoptosis induced by trophic factors withdrawal [31]. Similarly, activation of the death receptor pathway has been reported in rat brown adipocytes stimulated with tumour necrosis factor (TNF) α [32] triggering apoptotic cell death [32,33]. Interestingly, the expression of this pro-inflammatory cytokine is elevated in white adipose tissue (WAT) of a variety of obese animals [34] and humans [35] in parallel with a decrease in energy expenditure, thus reinforcing the connexion between inflammation, obesity and brown fat atrophy. In addition, there is growing evidence regarding the potential anti-inflammatory and anti-obesity benefits of natural phytochemicals such as resveratrol. It has been recently reported that this compound promotes apoptosis in 3T3-L1 cells and human white adipocytes [36,37], and this prompted us to investigate the effect of resveratrol on the viability of brown fat cells and a possible role of PTP1B in mediating its effects. In the current study we have found first a beneficial effect of PTP1B deficiency on brown fat adipogenesis by reducing the apoptotic rate during the induction phase of differentiation and, second, a protection of PTP1B $^{-/-}$ differentiated brown adipocytes against apoptosis induced by pro- and anti-inflammatory stimuli.

2. Materials and methods

2.1. Reagents and antibodies

Fetal serum and culture media were obtained from Invitrogen. Insulin, albumin, anti-beta-actin (A-5441) antibody and Oil Red O dye were from Sigma Chemical CO. (St. Louis, MO, USA). Protein A-agarose

was from Roche Molecular Biochemicals (Barcelona, Spain). The anti-IRS-3 antibody was a generous gift of MF White (Boston, MA). The anti-Large T antigen (LTAg) antibody was kindly provided by J. de Caprio, Dana Farber Cancer Institute (Boston, MA). The anti-IRS-1 (06-248), anti-phospho-IRS-1 (Ser307) (07-247), anti-PTP1B (07-088) and anti-Tyr(P) (clone 4G10, 05-321) antibodies were purchased from Upstate Biotechnology (Lake Placid, NY). Antibodies against Akt (#9272), phospho-Foxo1 (Ser256 # 9461), Foxo1 (#9462), cleaved (Asp175) caspase-3 (#9661), phospho-ERK1/2 (Thr202/Tyr204 #9101), and ERK1/2 (#9102) were purchased from Cell Signalling (Beverly, MA, USA). The anti-GLUT-4 (AB 1346) antibody was purchased from Chemicon (Chemicon International, CA, USA). The anti-C/EBP α (sc-61), anti-Mcl-1 (sc-819), anti-LysAc Foxo1 (clone 4G12, 05-515), anti-phospho-Akt (Ser473 sc-7985), anti-nucleolin (C23, MS-3; sc-8031), and anti-caveolin-1 (sc-894) antibodies were purchased from Santa Cruz Biotechnology (Palo Alto, CA, USA). Anti-Bim (Ref. 559685) and anti-Bcl x_L (Ref. 610211) antibodies were from BD Biosciences PharMingen (San Diego, CA). Anti-Bid (Ref. AF860) and anti-FLIP (Ref. AF821) antibodies were from R&D Systems. All other reagents used were of the purest grade available.

2.2. Generation of immortalized brown preadipocyte cell lines

Brown adipocytes were obtained from interscapular brown adipose tissue of 3–5 day-old wild-type (PTP1B $^{+/+}$) and PTP1B $^{-/-}$ neonatal mice and submitted to collagenase dispersion as previously described [38]. Brown preadipocytes were cultured in Dulbecco's modified Eagle's medium (DMEM) supplemented with 20% FS, 20 mM HEPES, and 100 U/ml penicillin/streptomycin until they reached 50–60% confluence. Viral Bosc-23 packaging cells were transfected at 70% confluence by calcium phosphate coprecipitation with 3 μ g/6 cm-dish of the puromycin-resistance retroviral vector pBabe encoding attenuated SV40 Large T antigen (kindly provided by J. de Caprio, Dana Farber Cancer Institute, Boston, MA). Then, primary brown preadipocytes were infected at 60% confluence with polybrene (4 μ g/ml)-supplemented virus for 48 h and maintained in culture medium for 72 h, before selection with puromycin (1 μ g/ml) for 2 weeks. Four or five different pools from each genotype, generated in independent infections, were expanded. All experiments were performed in two different pools of infected cells of either genotype.

PTP1B $^{-/-}$ immortalized neonatal preadipocytes were infected with retroviral murine wild-type PTP1B (kindly provided by ML Tremblay, McGill Cancer Center, Quebec, Canada) or empty vector as a control. After 48 h, cells were cultured in medium supplemented with hygromycin B (200 μ g/ml) and 3 different clones from each genotype were expanded. The expression of PTP1B in the different clones of infected cells was assessed by Western blotting. All experiments were performed in three independent clones from each genotype.

2.3. Differentiation of brown preadipocytes

For differentiation, immortalized brown preadipocytes were grown in DMEM supplemented with 10% FS, 20 nM insulin and 1 nM T3 (differentiation medium, DM) until reaching confluence. Next, the cells were cultured for two days in induction medium (IM) consisting of differentiation medium supplemented with 0.5 μ M dexamethasone, 0.125 μ M indomethacin and 0.5 mM isobutylmethylxanthine (IBMX). Then, cells were cultured in DM until day that exhibited a fully differentiated phenotype with numerous multilocular lipid droplets in their cytoplasm.

2.4. Oil Red O Staining

Dishes were washed once with phosphate-buffered saline and fixed with 10% buffered formalin for at least 16 h at 4 °C. Cells were then stained for 4 h at room temperature with Oil Red O solution

(5 g/l in isopropyl alcohol), washed three times with water, and visualized.

2.5. Analysis of IRA and IRB isoforms by semiquantitative PCR

To analyze endogenous IR isoforms in immortalized brown pre- and differentiated adipocytes, 5 µg of total RNA was primed with oligodT (deoxythymidine) in the presence of Murine Mammary Tumor Virus reverse transcriptase (Invitrogen) to synthesize cDNA. The samples were diluted 5-fold, and 5% of the total volume was used for subsequent PCR. Primers used were: mouse IR exon 11, primer 1, 5'-ATCAGAGTGAGTATGACGACTCGG-3'; and, primer 2, 5'-TCCTGACTTGT-GGGCACAAATGGTA-3'; human IR exon 11, primer 1, 5'-ACCAGAGTGAG-TATGAGGATTGG-3', primer 2, 5'-TCCGGACTCGTGGGCACGCTGGTC-3'. PCR reactions were resolved on 2% agarose gels.

2.6. Induction of apoptosis in differentiated brown adipocytes

Differentiated brown adipocytes (day 6) were stimulated with 10 nM TNF α plus 10 µg/ml cycloheximide (CHX) for 1–6 h, or with resveratrol (50–100 µM) for 16 h. At the end of the culture time, cells were collected and apoptosis was analyzed.

2.7. Immunoprecipitation

Differentiated brown adipocytes were treated with the apoptotic stimuli as described above. At the end of the experiments, cells were lysed at 4 °C in buffer containing 10 mM Tris-HCl, 5 mM EDTA, 50 mM NaCl, 30 mM disodium pyrophosphate, 50 mM NaF, 100 µM Na₃VO₄, 1% Triton X-100, 1 mM phenylmethylsulfonyl fluoride, 10 µg/ml leupeptin and 10 µg/ml aprotinin pH 7.6 (lysis buffer). After protein content determination, equal amounts of protein were immunoprecipitated at 4 °C with the corresponding antibodies. The immune complexes were collected on Protein A-agarose or antimouse IgG-agarose beads. Immunoprecipitates were washed with lysis buffer and analyzed by SDS-PAGE followed by Western blotting.

2.8. Western blotting

To obtain total cell lysates, cells from supernatants were collected by centrifugation at 2,000×g for 5 minutes at 4 °C. Attached cells were scraped off in ice-cold PBS, pelleted by centrifugation at 4,000×g for 10 min at 4 °C and resuspended in lysis buffer. Samples were sonicated for 30 seconds at 1.5 mA and lysates were clarified by centrifugation at 12,000×g for 10 minutes. After SDS-PAGE, proteins were transferred to Immobilon membranes and were blocked using 5% non-fat dried milk or 3% bovine serum albumin (BSA) in 10 mM Tris-HCl, 150 mM NaCl pH 7.5, and incubated overnight with the antibodies indicated in 0.05% Tween-20, 10 mM Tris-HCl, 150 mM NaCl pH 7.5. Immunoreactive bands were visualized using the ECL Western blotting protocol (Millipore).

2.9. Immunofluorescence and confocal imaging

Cells were grown, differentiated and further stimulated with resveratrol (100 µM) on glass coverslips, fixed in 4% paraformaldehyde for 15 min and processed for immunofluorescence. Anti-Foxo1 primary antibody (diluted 1:100) was applied for 1 h at 37 °C in PBS/1% BSA. The secondary antibody (Cy3-conjugated goat anti-rabbit, diluted 1:500) was applied for 30 min. Immunofluorescence was examined under an MRC-1024 (Bio-Rad, Hemel Hempstead, UK) confocal microscope adapted to an inverted Nikon Eclipse TE 300 microscope. Images were taken with 514-nm laser excitation and fluorescence emissions were detected through a 605/15-nm bandpass filter.

2.10. Quantification of apoptotic cells by flow cytometry

After induction of apoptosis, adherent and non-adherent cells were collected by centrifugation, washed with PBS and fixed with cold ethanol (70% vol/vol). The cells were then washed, resuspended in PBS and incubated with RNase A (25 µg/10⁶ cells) for 30 min at 37 °C. After addition of 0.05% propidium iodide, cells were analyzed by flow cytometry.

2.11. Analysis of caspase-3 activity

Cells were scraped off, collected by centrifugation at 2,500 × g for 5 minutes and lysed at 4 °C in 5 mM Tris/HCl pH 8, 20 mM EDTA, 0.5% Triton X-100. Lysates were clarified by centrifugation at 13,000 × g for 10 min. Reaction mixtures contained 25 µl cell lysate, 325 µl assay buffer (20 mM HEPES pH 7.5, 10% glycerol, 2 mM dithiothreitol) and 20 µM caspase-3 substrate (Ac-DEVD-AMC). After 2 h incubation in the dark, enzymatic activity was measured in a luminescence spectrophotometer (Perkin Elmer LS-50, Norwalk, CT) (λ excitation, 380 nm; λ emission, 440 nm). We define a unit of caspase-3 activity as the amount of active enzyme necessary to produce an increase in 1 arbitrary unit in the fluorimeter after 2-hour incubation with the reaction mixture. Then, protein concentration of cell lysates was determined, and the results are presented as caspase-3 activity/µg of total protein.

2.12. Analysis of caspase-8 activity

Cells were scraped off, collected by centrifugation and lysed as described for caspase-3 activity. Caspase-8 activity was measured with the ApoAlert Caspase-8 fluorescent assay kit (Clontech, Ref. K2028) according to the manufacturer's instructions using IETD-AFC as a substrate. Then, protein concentration of cell lysates was determined, and the results are presented as caspase-8 activity/µg of total protein.

2.13. Statistical analysis

Statistically significant differences between mean values were determined using Student's paired t test. Differences were considered statistically significant at p < 0.05.

3. Results

3.1. PTP1B deficiency accelerates brown adipocyte differentiation

To investigate whether PTP1B affects brown adipocyte differentiation, we generated immortalized brown preadipocyte cell lines from wild-type (PTP1B^{+/+}) and PTP1B^{-/-} neonatal mice. As shown in Fig. 1A, all PTP1B^{-/-} brown adipocyte cell lines lacked PTP1B expression and expressed similar levels of LTag as the wild-type controls. Next, postconfluent brown preadipocytes were submitted to the differentiation protocol using insulin, T3, IBMX, dexamethasone, and indomethacin, as described in Materials and Methods. Fig. 1B shows substantial differences in the time-course and the intensity of Oil Red O staining between both genotypes. At day 5, PTP1B^{-/-} brown adipocytes displayed a fully differentiated phenotype (Fig. 1B, lower row). By contrast, wild-type cells reached maximal Oil Red O staining at day 6 (Fig. 1B, upper row). Moreover, in these cells the intensity of the staining was significantly lower than in differentiated brown adipocytes lacking PTP1B. Next, we analyzed possible differences between both genotypes of brown fat cells in the expression of adipogenic and thermogenic markers during the time-course of differentiation. Regarding thermogenesis, PTP1B^{-/-} brown adipocytes (Fig. 1C, right panels) expressed higher levels of UCP-1 than the wild-type controls (Fig. 1C, left panels). Indeed, its coactivator PGC-1α

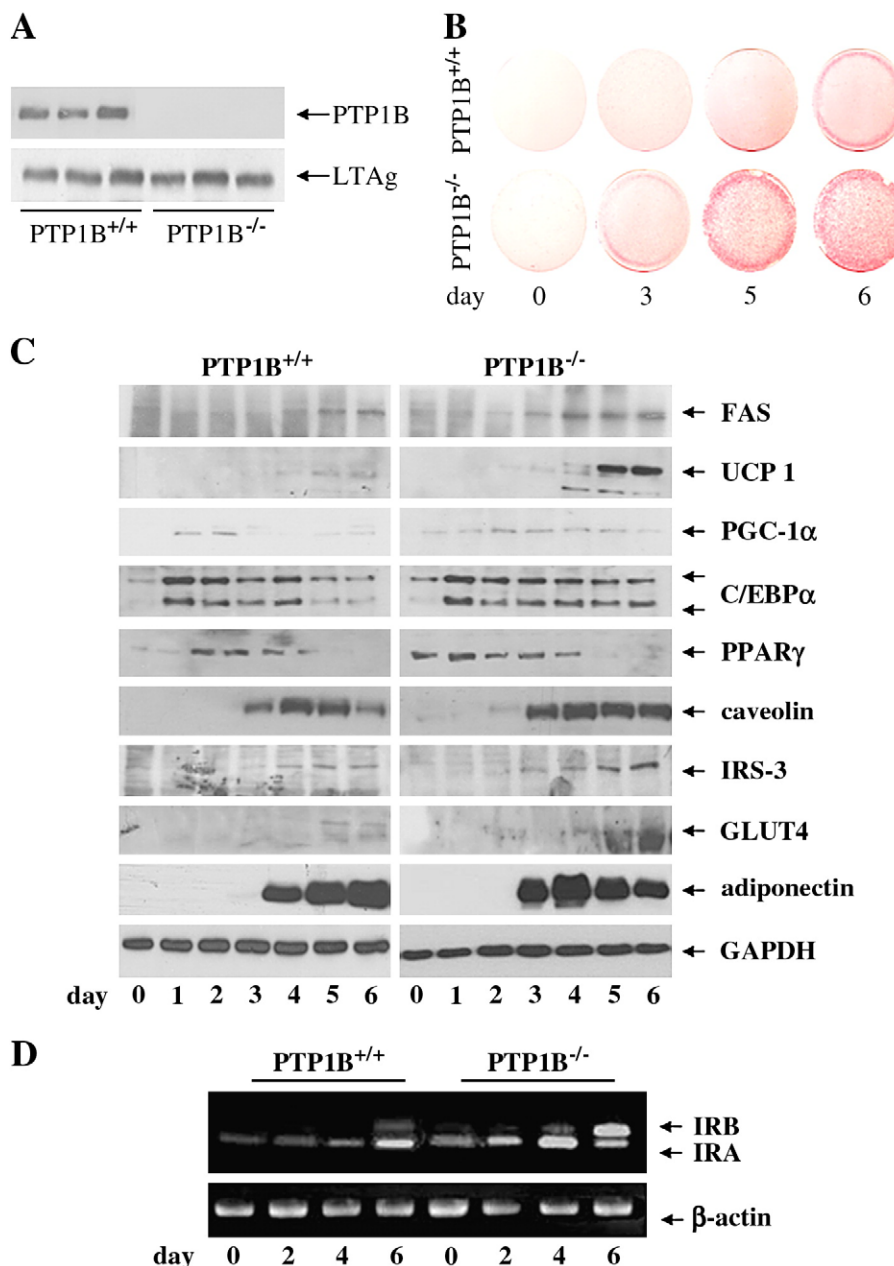


Fig. 1. PTP1B deficiency accelerates and enhances brown adipocyte differentiation. **A.** Immortalized wild-type (PTP1B^{+/+}) and PTP1B^{-/-} preadipocyte cell lines were generated as described in Materials and Methods. The expression of PTP1B and Large T antigen (LTA) was analyzed by Western blot in three different pools of immortalized cells. **B.** Brown preadipocytes were grown until confluence and differentiated into adipocytes as described in Materials and Methods. Cells were fixed and stained with Oil Red O. A representative experiment is shown. **C.** Protein expression of brown adipocyte differentiation markers in PTP1B^{+/+} and PTP1B^{-/-} cells on days 0 to 6. Whole cell lysates were prepared and analyzed for FAS, C/EBP α , PPAR γ , GLUT4, caveolin, adiponectin, IRS-3, UCP1 and PGC-1 α expression by Western blot. The results are representative of two independent experiments performed in different pools of immortalized cells. **D.** RNA was isolated from PTP1B^{+/+} and PTP1B^{-/-} brown preadipocytes (day 0) and differentiating brown adipocytes at the indicated days, and RT-PCR was performed as described in Materials and Methods. As a loading control RT-PCR with mouse β -actin primers was performed. A representative experiment is shown.

peaked at day 2 in both kinds of brown adipocytes, but whereas PGC-1 α levels declined at day 3 in wild-type cells, in brown adipocytes lacking PTP1B its expression was sustained until day 6. Next, we monitored the expression of adipogenic markers such as C/EBP α , PPAR γ , GLUT4 and FAS. C/EBP α was expressed at low but detectable levels in preadipocytes (day 0) with both genotypes and rose dramatically in cells undergoing differentiation, peaking at day 1. In wild-type cells, its expression declined at day 5 whereas in PTP1B^{-/-} cells it was prolonged until day 6. PPAR γ also peaked at day 2 in wild-type differentiating cells but, notably, its expression was already up-regulated in PTP1B^{-/-} brown preadipocytes before differentiation; its

expression declined at day 5 in both cell types. Levels of the insulin-responsive glucose transporter GLUT4 reached a maximum at day 5 in cells with either genotype, but were substantially higher in the absence of PTP1B. Likewise, IRS-3, a member of the IRS family exclusively expressed in differentiated adipocytes, was maximally expressed at day 6 in PTP1B^{-/-} brown adipocytes, reaching higher levels than in the wild-type controls. We have previously reported that IRS-3 and caveolin-1 colocalize in caveolae-enriched structures in differentiated brown adipocytes [39]. Accordingly, levels of caveolin-1 were higher in differentiating PTP1B^{-/-} brown adipocytes than in the wild-type controls. In addition, brown adipocytes expressed the insulin-

sensitizing adipokine adiponectin [40]. During differentiation, adiponectin expression was detected at day 4 in wild-type brown adipocytes, whereas in PTP1B^{-/-} cells its expression was highly detectable at day 3. Finally, we monitored the differentiation of wild-type and PTP1B^{-/-} brown adipocytes by the analysis of the expression profile of the insulin receptor (IR) isoforms IRA (-exon 11) and IRB (+exon 11). In brown preadipocytes from both genotypes (day 0), the IRA isoform was predominant (Fig. 1D). During differentiation there was a gradual increase in the IRB isoform, as reported by Entight et al. [41]. However, the IRB isoform was consistently expressed at higher levels and at an early time (day 4) in differentiating PTP1B^{-/-} brown adipocytes than in the wild-type controls. Altogether these results indicate a beneficial effect of PTP1B deletion on brown adipocyte differentiation.

3.2. Differentiated PTP1B-deficient brown adipocytes exhibit insulin hypersensitivity

Although the insulin hypersensitivity of PTP1B-deficient mice has been reported, the insulin responsiveness of fully differentiated brown adipocytes lacking this phosphatase remains unknown. Differentiated brown adipocytes (day 6) from both genotypes were serum starved for 15 h and further stimulated with insulin (1 or 10 nM) for 10 min. Then, insulin sensitivity was monitored by the phosphorylation of Akt/PKB. As shown in Fig. 2A, maximal Akt/PKB phosphorylation was elicited at 1 nM in PTP1B^{-/-} cells, whereas wild-type controls responded maximally to insulin at the 10 nM dose. Next, we explored whether conditioned medium collected from differentiated brown adipocytes lacking or expressing PTP1B could differentially affect insulin sensitization of a different insulin target cell type. For this goal human liver (Chang liver, CHL) cells were cultured for 16 h in conditioned medium from wild-type or PTP1B^{-/-} brown adipocytes collected at day 4 of differentiation, time at which substantial differ-

ences in the expression of differentiation markers were observed (see Fig. 1C,D). Then, human liver cells were deprived of conditioned medium for 4 h and further stimulated with insulin (10 nM) for 10 min. Human liver cells pre-incubated with conditioned medium from wild-type brown adipocytes showed increased Akt/PKB phosphorylation compared to liver cells cultured in DMEM-10% FS (Fig. 2B). Interestingly, the insulin sensitizing effect was stronger when human liver cells were incubated with conditioned medium from differentiated brown adipocytes lacking PTP1B.

3.3. PTP1B-deficient brown preadipocytes are protected against apoptosis during the induction phase of differentiation

In white adipocyte differentiation, re-entry into the cell cycle of growth-arrested preadipocytes is known as the clonal expansion phase [42]. By contrast, knowledge of the early events of brown adipocyte differentiation is still very limited. As reported by us and others [20,24], postconfluent brown preadipocytes (day 0) were cultured for 48 h in induction medium containing a cocktail of insulin, T3, dexamethasone, IBMX and indomethacin. During this time, known as the induction phase, phase-contrast microscopy revealed many wild-type brown adipocytes with morphological characteristics of apoptotic cells (not shown). This prompted us to analyze the percentage of apoptotic cells, the survival signalling and the balance between pro- and anti-apoptotic proteins during the induction phase of brown adipocyte differentiation. As depicted in Fig. 3A (upper panel), the percentage of hypodiploid wild-type brown adipocytes increased by threefold and fivefold after 24 and 48 h of induction, respectively, and then decreased coincident with the withdrawal of the induction medium. Moreover, activation of the executor caspase-3 was maximal 24 h after induction and remained elevated at 48 h, declining to basal levels at day 3 (Fig. 3A, lower panel). As we and

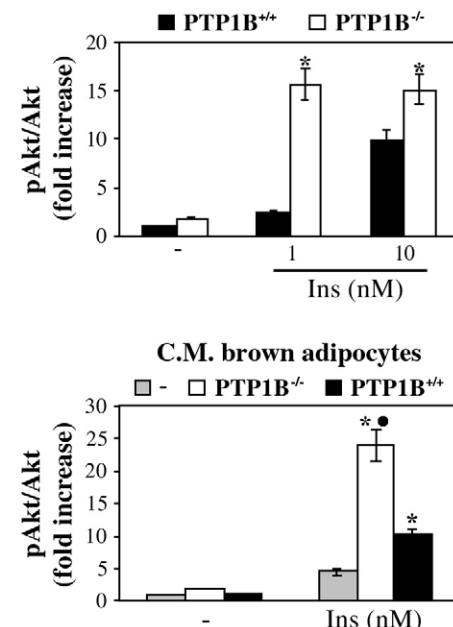
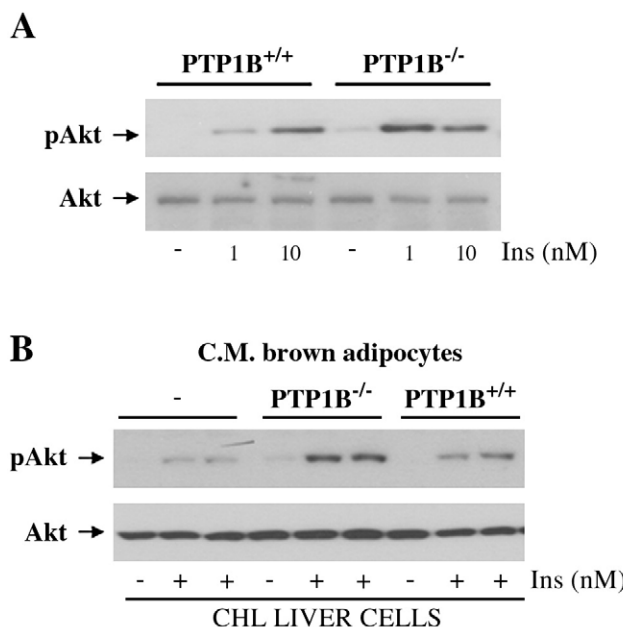


Fig. 2. Differentiated PTP1B^{-/-} brown adipocytes exhibit insulin hypersensitivity. A. Differentiated PTP1B^{+/+} and PTP1B^{-/-} brown adipocytes were serum-starved for 15 h and stimulated with 1 or 10 nM insulin for 10 min. At the end of the culture time, brown adipocytes were harvested and whole cell lysates were prepared. Total protein (50 µg) was analyzed by Western blot using anti-phospho-Akt (ser-473) and anti-Akt specific antibodies. Autoradiograms of three independent experiments were quantified by scanning densitometry. Results are expressed as fold increase of Akt phosphorylation by insulin and are means ± SE. *p < 0.05, PTP1B^{-/-} versus PTP1B^{+/+}. B. PTP1B^{+/+} and PTP1B^{-/-} brown adipocytes were submitted to the differentiation protocol. At day 4, medium was removed. Human Chang liver cells (CHL) were grown to 80% confluence in DMEM plus 10% FCS (growing medium), and then incubated for 16 h with conditioned medium from PTP1B^{+/+} or PTP1B^{-/-} brown adipocytes (obtained at day 4 of differentiation) or left in growing medium. Next, CHL cells were serum-deprived for 4 h and stimulated with 10 nM insulin for 10 min. Total protein was analyzed by Western blot using anti-phospho-Akt (ser-473) and anti-Akt specific antibodies. Autoradiograms from three independent experiments were quantified by scanning densitometry. Results are expressed as fold increase of Akt phosphorylation by insulin and are means ± SE. *p < 0.05, CHL cells cultured with the conditioned medium obtained from PTP1B^{+/+} or PTP1B^{-/-} versus CHL cells cultured with DMEM 10% FS. • p < 0.05, CHL cells cultured with the conditioned medium obtained from PTP1B^{-/-} versus CHL cells cultured with the conditioned medium obtained from PTP1B^{+/+}.

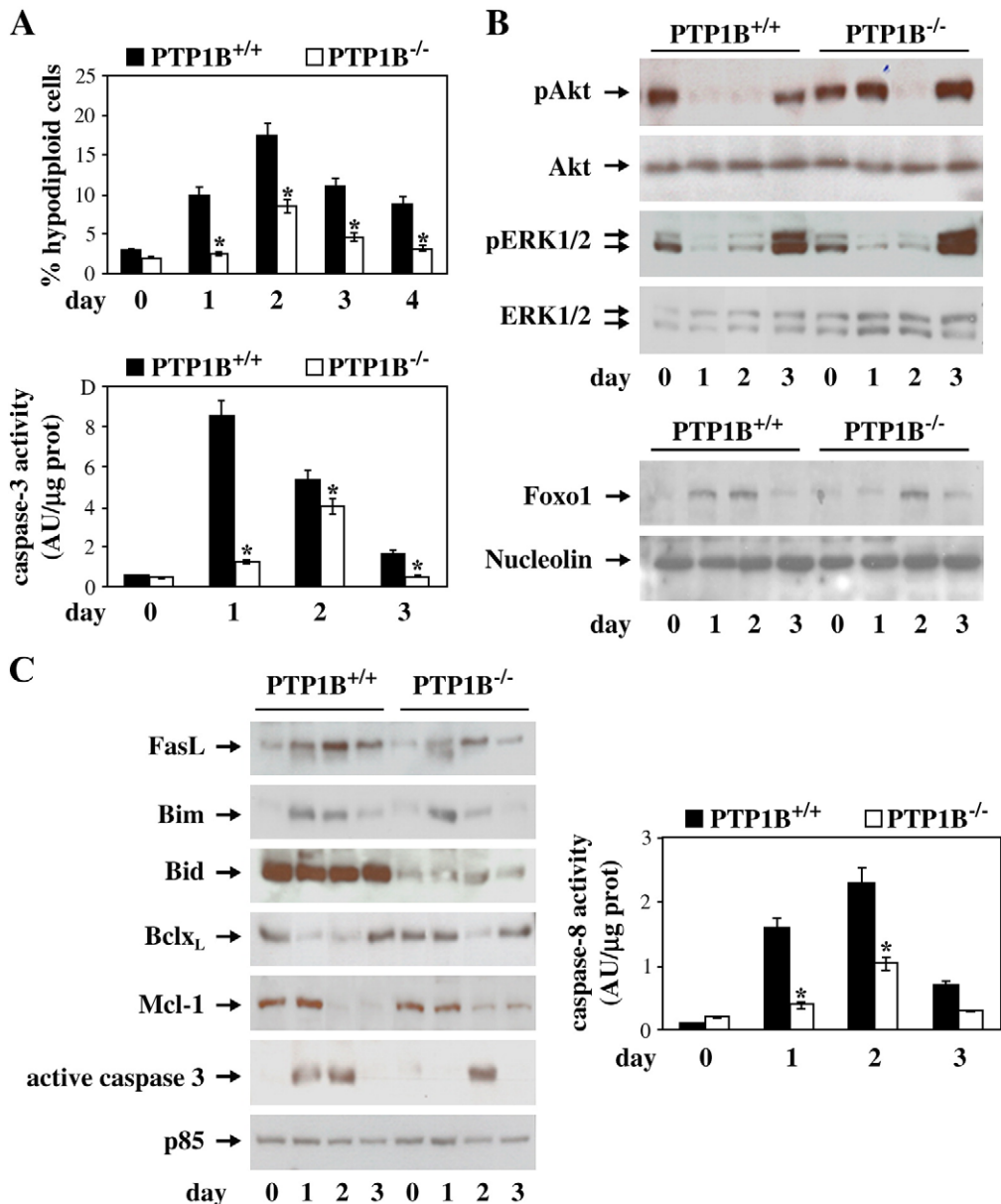


Fig. 3. PTP1B^{-/-} brown preadipocytes are protected against programmed cell death during clonal expansion. **A.** (upper panel) PTP1B^{+/+} and PTP1B^{-/-} brown preadipocytes were induced to differentiate and at the times indicated cells were trypsinized and fixed. The percentage of cells with DNA lower than 2C (apoptotic cells) was determined by flow cytometry. Results are expressed as percentage of apoptotic cells and are means \pm SE from three independent experiments. *p < 0.05, PTP1B^{-/-} versus PTP1B^{+/+}. (lower panel) Caspase-3 enzymatic activity was measured in differentiating PTP1B^{+/+} and PTP1B^{-/-} brown preadipocytes. Results are expressed as arbitrary units/ug protein and are means \pm SE from three independent experiments. *p < 0.05, PTP1B^{-/-} versus PTP1B^{+/+}. **B.** (upper panel) Whole cell extracts were prepared from differentiating brown preadipocytes and subjected to immunoblotting with antibodies against phospho-Akt (ser-473), Akt, phospho-ERK1/2 (Thr202/Tyr204) and total ERK1/2. (lower panel) Nuclear protein (50 μ g) was submitted to Western blot analysis with the anti-Foxo1 antibody. Nucleolin was used as a loading control. A representative experiment is shown. **C.** (left panel) Whole cell extracts were prepared from differentiating brown preadipocytes and subjected to immunoblotting with antibodies against FasL, Bim, Bid, Bclx_L, Mcl-1, active caspase-3 and p85 α -PI 3-kinase for protein loading. A representative experiment of three is shown. (right panel) Caspase-8 enzymatic activity was measured in differentiating PTP1B^{+/+} and PTP1B^{-/-} brown preadipocytes. Results are expressed as arbitrary units/ug protein and are means \pm SE from three independent experiments. *p < 0.05, PTP1B^{-/-} versus PTP1B^{+/+}.

others have shown that PTP1B deficiency protects insulin target cells against programmed cell death [30,31], we analyzed these apoptotic parameters in PTP1B^{-/-} brown fat cells. Fig. 3A shows that in differentiating PTP1B^{-/-} brown adipocytes the peak of hypodiploid cells was delayed as compared to the wild-type controls, being undetectable at 24 h post-induction but reaching a threefold increase at 48 h, time at which caspase-3 was maximally activated. In light of these results, we examined the activation of Akt/PKB and ERK1/2 that trigger survival signals in multiple mammalian cell types [43]. Whereas phosphorylation of Akt/PKB was down-regulated in wild-type differentiating brown adipocytes 24 h after induction (Fig. 3B), in

differentiating PTP1B^{-/-} brown adipocytes it remained high at 24 h but it was down-regulated at 48 h post-induction. Notably, Akt/PKB phosphorylation was recovered at day 3 in both cell types. It is well known that Akt/PKB phosphorylates the transcription factor Foxo1, thereby precluding its entry into the nucleus [44]. Accordingly, in this study we assessed the modification of the sub-cellular distribution of Foxo1 as a possible mechanism by which PTP1B levels might modulate apoptosis in differentiating brown adipocytes. In the undifferentiated state (day 0), Foxo1 content was almost undetectable in nuclear extracts from either cell line (Fig. 3B). However, substantial differences were noted following induction. Whereas Foxo1 was

present in nuclear extracts 24 h post-induction in wild-type cells, it was not detected in PTP1B^{-/-} cells. Of note, nuclear Foxo1 was present in differentiating PTP1B^{-/-} adipocytes only 48 h post-induction. All nuclear fractions were assumed to be pure, as cytosolic p85α was not detected by Western blotting of these preparations (not shown). In parallel with the recovery of Akt/PKB phosphorylation, Foxo1 was not detected in nuclear extracts at day 3 in both wild-type and PTP1B^{-/-} differentiating brown adipocytes. Regarding ERK1/2 phosphorylation, a substantial down-regulation was observed in both cell types at 24–48 h post-induction with a total recovery at day 3.

In an attempt to elucidate the molecular basis for the protection against apoptosis during the early phases of differentiation in brown adipocytes lacking PTP1B, we studied the expression of pro- and anti-apoptotic proteins that are implicated in the death receptor (extrinsic) and mitochondrial (intrinsic) pathways. Particularly, we analyzed Bim and FasL levels because these proteins are Foxo1 targets [45,46]. Both FasL and Bim levels were low in preadipocytes with either genotype. However, a marked increase in these proteins was detected in wild-type brown adipocytes at 24–48 h post-induction, declining at day 3 (Fig. 3C). By contrast, in cells lacking PTP1B the expression of FasL

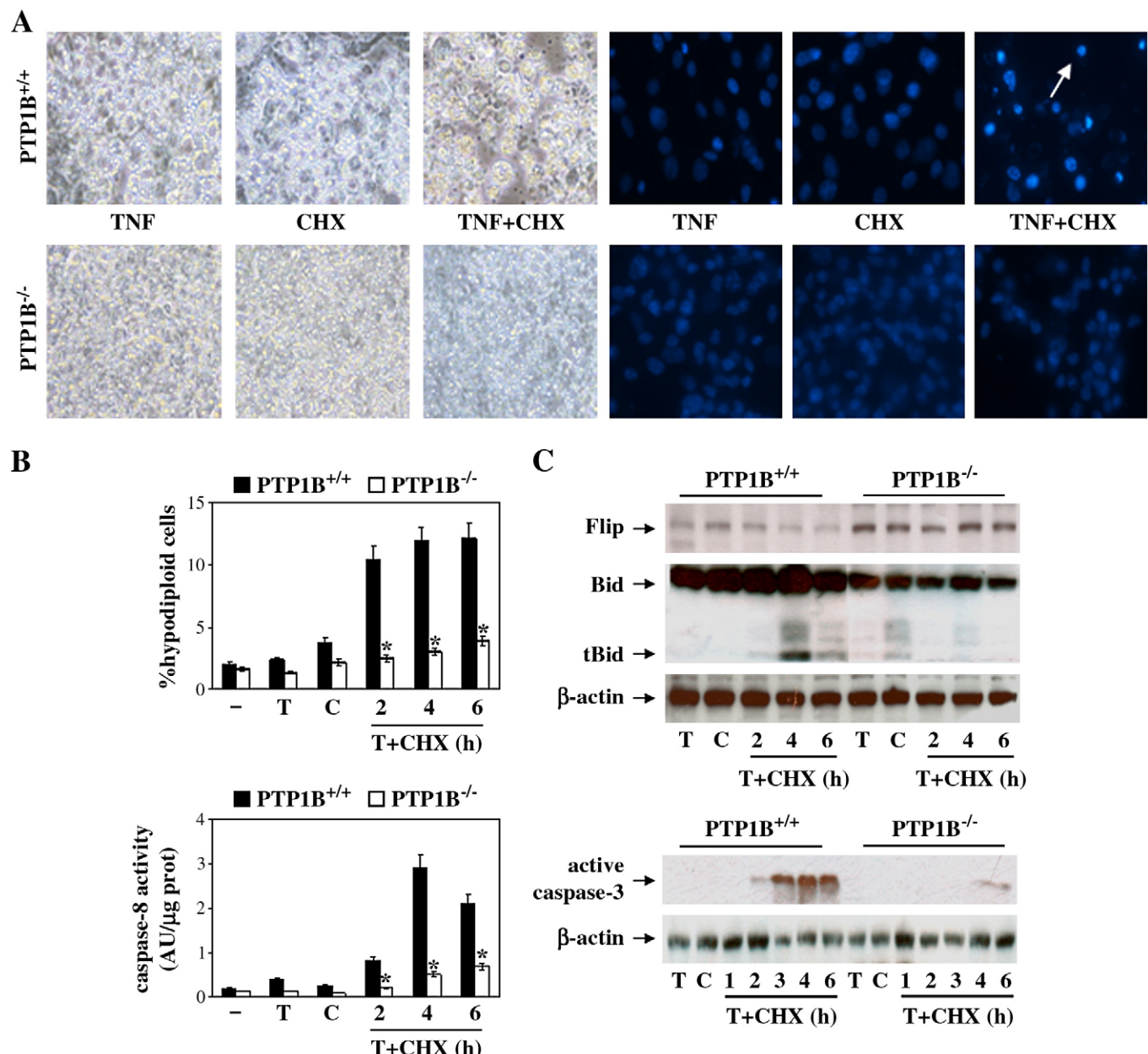


Fig. 4. PTP1B^{-/-} brown adipocytes are resistant to the activation of the TNFα-induced death receptor apoptotic pathway. **A.** (left panels) Differentiated PTP1B^{+/+} and PTP1B^{-/-} brown adipocytes were stimulated with TNFα (10 nM), CHX (10 μg/ml), or TNFα plus CHX (T+CHX) for 5 h. Representative phase-contrast micrographs are shown. (right panels) Representative images of the nuclear morphology of untreated and treated PTP1B^{+/+} and PTP1B^{-/-} brown adipocytes after staining of DNA with DAPI and visualization by fluorescence microscopy. The arrow points to a fragmented nucleus. **B.** (upper panel) Differentiated PTP1B^{+/+} and PTP1B^{-/-} brown adipocytes were stimulated as described above for the indicated time periods. The percentage of cells with DNA lower than 2C (apoptotic cells) was determined by flow cytometry. Results are expressed as percentage of apoptotic cells are means ± SE from three independent experiments. *p < 0.05, PTP1B^{-/-} versus PTP1B^{+/+}. (lower panel) Caspase-8 enzymatic activity was measured in differentiating PTP1B^{+/+} and PTP1B^{-/-} brown preadipocytes. Results are expressed as arbitrary units/μg protein and are means ± SE from three independent experiments. *p < 0.05, PTP1B^{-/-} versus PTP1B^{+/+}. **C.** Cells were stimulated as described in A. Total protein extracts were analyzed by immunoblotting with antibodies against FLIP, Bid, active caspase-3 and β-actin as a loading control. Similar results were obtained in three independent experiments.

remained low at 24 h post-induction but it was slightly elevated after 48 h. As a result, caspase-8 enzymatic activity was higher in 24–48 h differentiating wild-type brown adipocytes as compared to PTP1B^{-/-} cells. Conversely, Bim was up-regulated 24–48 h post-induction as in wild-type brown adipocytes, suggesting that in differentiating brown adipocytes Foxo1-independent mechanisms might modulate Bim expression. Of note, Bid expression was constitutively down-regulated in brown preadipocytes lacking PTP1B and did not change upon induction of differentiation. Finally, we analyzed the expression of Bclx_L and Mcl-1, two anti-apoptotic members of the Bcl-2 family. In parallel with Akt/PKB phosphorylation, Bclx_L was down-regulated in wild-type brown preadipocytes 24–48 h post-induction but it was completely recovered at day 3. However, in PTP1B^{-/-} brown adipocytes Bclx_L down-regulation was delayed until 48 h post-induction. Regarding Mcl-1, its expression was decreased at 48 h in both cell types, but the decrease was clearly more pronounced in PTP1B^{+/-} cells. Altogether these results indicate that in brown adipocytes the imbalance between pro- and anti-apoptotic proteins during induction of differentiation was less severe in the absence of PTP1B.

3.4. Fully differentiated PTP1B-deficient brown adipocytes are protected against activation of the TNF α -induced death receptor apoptotic pathway

The expression of TNF α is elevated in WAT of a variety of obese animals and humans [34,35]. Importantly, this pro-inflammatory cytokine has been shown to induce apoptosis in rat brown adipocytes [32,33]. To investigate whether PTP1B deficiency affects TNF α -induced apoptosis, we compared the effect of death receptor activation in fully differentiated wild-type and PTP1B^{-/-} brown adipocytes. For this goal cells were stimulated with TNF α (10 nM), CHX (10 μ g/ml), or TNF α plus CHX for 5 h. Phase-contrast microscopy revealed that neither TNF α nor CHX alone induced apoptosis in brown adipocytes, regardless of PTP1B expression (Fig. 4A, left panel). However, the combination of both stimuli induced apoptosis in PTP1B^{+/-} brown adipocytes, but brown adipocytes lacking this phosphatase were resistant to the apoptotic effect of TNF α plus CHX. Analysis of nuclear morphology confirmed an increase in the incidence of condensed and/or fragmented nuclei in wild-type brown adipocytes treated with TNF α plus CHX (50%) in comparison to PTP1B^{-/-} cells (<10%) (Fig. 4A, right panel). These results suggest that in differentiated brown adipose cells there is a direct link between PTP1B expression and susceptibility to apoptosis upon TNF α receptor activation. Next, we measured the percentage of cells undergoing apoptosis by quantification of the hypodiploid peak. Treatment with TNF α plus CHX increased the percentage of hypodiploid wild-type brown adipocytes, reaching a maximal effect after 4 h (Fig. 4B, upper panel). However, this effect was significantly attenuated in the absence of PTP1B.

To determine the step in the extrinsic apoptotic cascade that is blocked as a result of PTP1B deficiency, we studied the activation of caspase-8. As shown in Fig. 4B (lower panel), activation of caspase-8 following TNFR oligomerization was abrogated in PTP1B^{-/-} brown adipocytes. Activation of caspase-8 is modulated by the levels of FLICE inhibitory protein (c-FLIP). Therefore, FLIP protein degradation is a key event in TNF α -induced cell death. In wild-type brown adipocytes stimulated with TNF α plus CHX, FLIP levels were consistently reduced after 2–6 h (Fig. 4C). Of note, degradation of FLIP was inhibited in PTP1B^{-/-} cells. As a result, detectable levels of tBid were observed in TNF α plus CHX-stimulated wild-type brown adipocytes, but not in PTP1B^{-/-} cells. Consistent with our previous data, cleavage of the executor caspase-3 following TNFR oligomerization was abrogated in PTP1B^{-/-} brown adipocytes.

3.5. The IRS-1/Akt/PKB survival signalling pathway is sustained in TNF α -stimulated PTP1B-deficient brown adipocytes

In brown adipocytes, IRS-1 plays a unique role in the activation of Akt/PKB which represents a major survival pathway in many mamma-

lian cells [38]. On that basis, we investigated IRS-1 tyrosine phosphorylation in TNF α plus CHX-treated brown adipocytes with either genotype. As depicted in Fig. 5A, IRS-1 tyrosine phosphorylation was high in wild-type brown adipocytes before apoptotic induction, and decreased dramatically upon 3 h of treatment with TNF α plus CHX. Conversely, PTP1B^{-/-} cells retained IRS-1 tyrosine phosphorylation even after 5 h of apoptotic stimulation. Under these conditions, IRS-1 degradation was detected in wild-type brown adipocytes, but in PTP1B^{-/-} cells this effect was attenuated. Since it has been shown that phosphorylation of IRS-1 on the ser-307 residue precedes its degradation [47], we analyzed the status of IRS-1 ser-307 phosphorylation under apoptotic and non-apoptotic conditions. IRS-1 ser-307 phosphorylation was hardly detectable in control non-apoptotic brown adipocytes but was transiently increased upon TNF α plus CHX treatment in cells from both genotypes. Besides, Akt/PKB phosphorylation was differentially regulated by TNF α plus CHX treatment. Whereas in wild-type brown adipocytes Akt/PKB phosphorylation declined after 4 h of apoptotic induction, it remained elevated in brown adipocytes lacking PTP1B (Fig. 5B). In parallel, the anti-apoptotic Bcl2 family member Bclx_L was down-regulated by TNF α plus CHX stimulation exclusively in wild-type brown adipocytes.

3.6. Resveratrol induces apoptosis in wild-type brown adipocytes by decreasing Akt/PKB phosphorylation and Foxo1 phosphorylation/acetylation: protection by PTP1B deficiency

Resveratrol (3,4',5-trihydroxy-trans-stilbene), a polyphenolic natural product, is a phytoalexin widely present in red wine and other constituents of the human diet (e.g. peanuts, grapes, and mulberries).

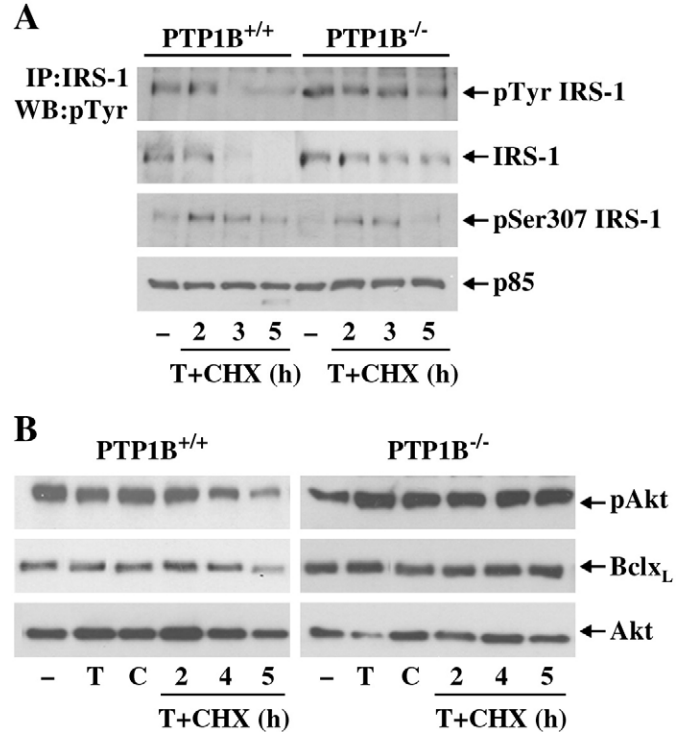


Fig. 5. Sustained activation of the IRS-1/Akt survival pathway in PTP1B^{-/-} brown adipocytes stimulated with TNF α plus CHX. A. Differentiated PTP1B^{+/-} and PTP1B^{-/-} brown adipocytes were stimulated with TNF α plus CHX (T + CHX) or left untreated for the indicated time periods. At the end of the culture time, cells were lysed and 600 μ g of total protein were immunoprecipitated with anti-pTyr antibody, and analyzed by Western blot with anti-IRS-1 antibody. Whole cell lysates were analyzed by Western blot with antibodies against IRS-1, phospho-IRS-1 (ser-307) and p85 α -PI 3-kinase as a loading control. Representative autoradiograms are shown. B. Apoptosis was induced as described above. At the end of the culture time cells were lysed and total protein extracts (50 μ g) were analyzed by Western blot with the antibodies against phospho-Akt (ser-473), total Akt and Bclx_L. A representative experiment of three is shown.

It exhibits anti-inflammatory properties by attenuating the expression and secretion of pro-inflammatory cytokines induced by TNF α in 3 T3-L1 adipocytes through activation of the histone deacetylase Sirt1 [48]. It has also been reported that resveratrol decreases proliferation and induces apoptosis and cell cycle arrest in various cell lines including 3 T3-L1 adipocytes [37]. On that basis, our next step was to investigate the apoptotic response to resveratrol in differentiated wild-type and PTP1B $^{-/-}$ brown adipocytes. Cells were stimulated with resveratrol at doses that induced apoptosis in 3 T3-L1 adipocytes (50 and 100 μ M) for 16 h. As observed with TNF α plus CHX treatment, phase-contrast microscopy revealed many wild-type brown adipocytes with morphological characteristics of apoptotic cells and the presence of condensed/fragmented nuclei 16 h after the addition of resveratrol (Fig. 6A). By contrast, neither changes in cellular morphology nor condensed/fragmented nuclei were observed in PTP1B $^{-/-}$ brown adipocytes in the presence of this compound. Moreover, the percentage of hypodiploid cells was significantly increased in resveratrol-treated wild-type brown adipocytes compared to PTP1B $^{-/-}$ cells (Fig. 6B). In light of these results, we investigated possible differences in pro- and anti-apoptotic signalling pathways upon resveratrol treatment in brown adipocytes from both genotypes. Whereas no differences in IRS-1 expression and its tyrosine phosphorylation were found between control and resveratrol-treated wild-

type and PTP1B $^{-/-}$ brown adipocytes (Fig. 7), Akt/PKB phosphorylation was significantly decreased only in wild-type cells. Downstream of Akt/PKB, the Foxo1 transcription factor was phosphorylated on ser-256 in untreated brown adipocytes with either genotype. However, PTP1B $^{-/-}$ cells retained Foxo1 ser-256 phosphorylation in the presence of resveratrol, whereas this phosphorylation decreased markedly in wild-type cells. Recently, it has been shown that activation of Sirt1 by resveratrol deacetylates Foxo1 and renders it immobile within the nuclear compartment, thereby promoting Foxo1-dependent transcription [49]. To explore whether this effect was modulated by PTP1B in brown adipocytes, we analyzed the acetylated state of Foxo1 upon resveratrol treatment. Fig. 7 shows that resveratrol decreased Foxo1 acetylation in wild-type, but not in PTP1B $^{-/-}$ brown adipocytes. Interestingly, this was coincident with its nuclear accumulation as shown by Western blot and immunofluorescence analysis (Fig. 8). As Bim and Bcl6, a transcriptional repressor of Bclx $_L$ [50], are Foxo1 targets, we analyzed the effect of resveratrol on Bclx $_L$ /Bim ratio. In wild-type brown adipocytes stimulated with resveratrol the expression of Bim was up-regulated whereas Bclx $_L$ was decreased (Fig. 7). Thus, the ratio Bclx $_L$ /Bim significantly decreased as compared to the controls. However, very low levels of Bim and high Bclx $_L$ expression were detected in resveratrol-treated PTP1B $^{-/-}$ brown adipocytes, and the Bclx $_L$ /Bim ratio remained similar to that observed in the untreated

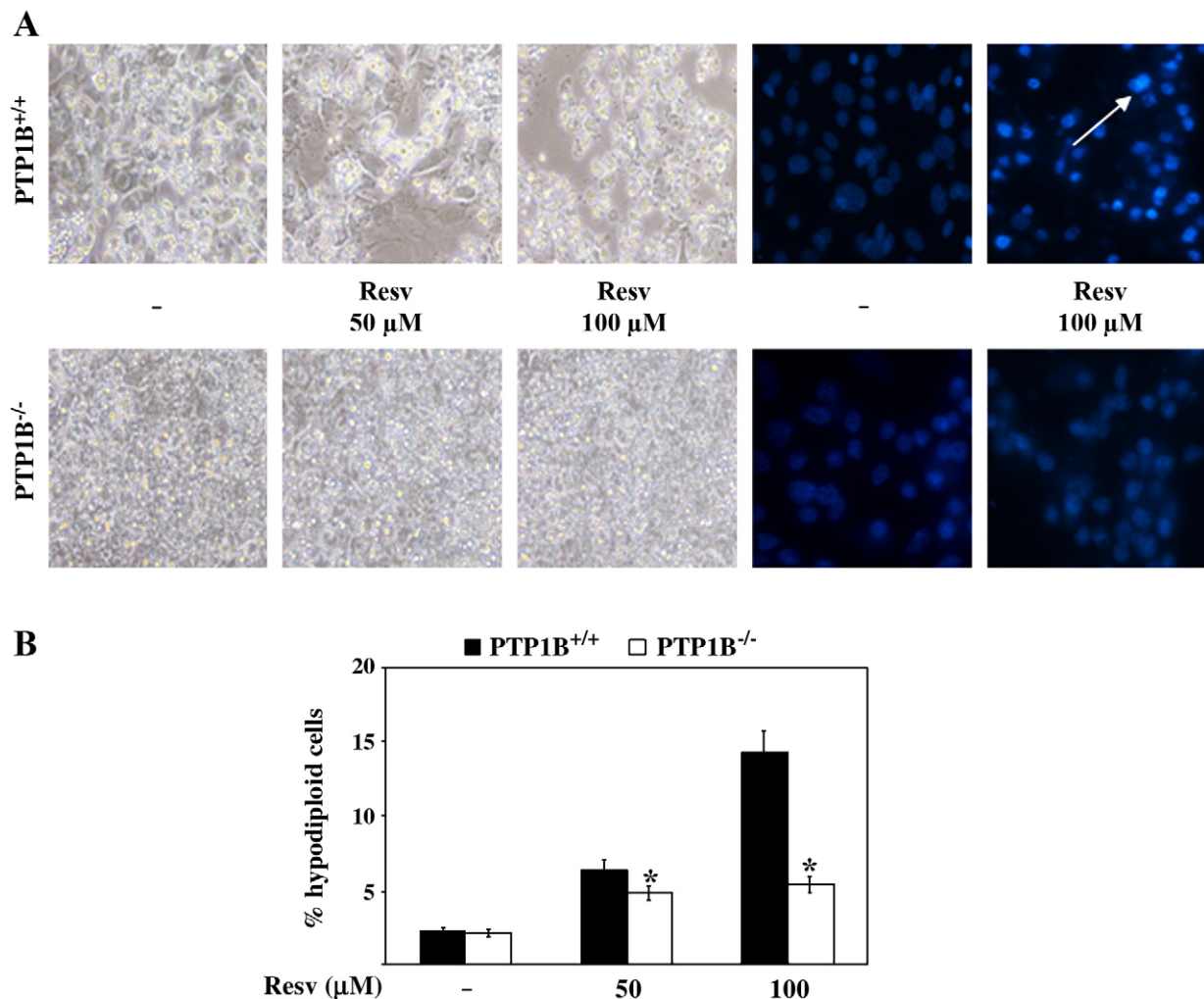


Fig. 6. Resveratrol induces apoptosis in wild-type brown adipocytes, but not in PTP1B $^{-/-}$ cells. A. (left panel) Differentiated PTP1B $^{+/+}$ and PTP1B $^{-/-}$ brown adipocytes were stimulated with resveratrol (50 or 100 μ M) for 16 h. Representative phase-contrast micrographs are shown. (right panel) Representative images of the nuclear morphology of untreated and treated PTP1B $^{+/+}$ and PTP1B $^{-/-}$ brown adipocytes after staining of DNA with DAPI and visualization by fluorescence microscopy. B. Differentiated PTP1B $^{+/+}$ and PTP1B $^{-/-}$ brown adipocytes were stimulated as described above. The percentage of cells with DNA lower than 2C (apoptotic cells) was determined by flow cytometry. Results are expressed as percentage of apoptotic cells are means \pm SE from three independent experiments. *p < 0.05, PTP1B $^{-/-}$ versus PTP1B $^{+/+}$.

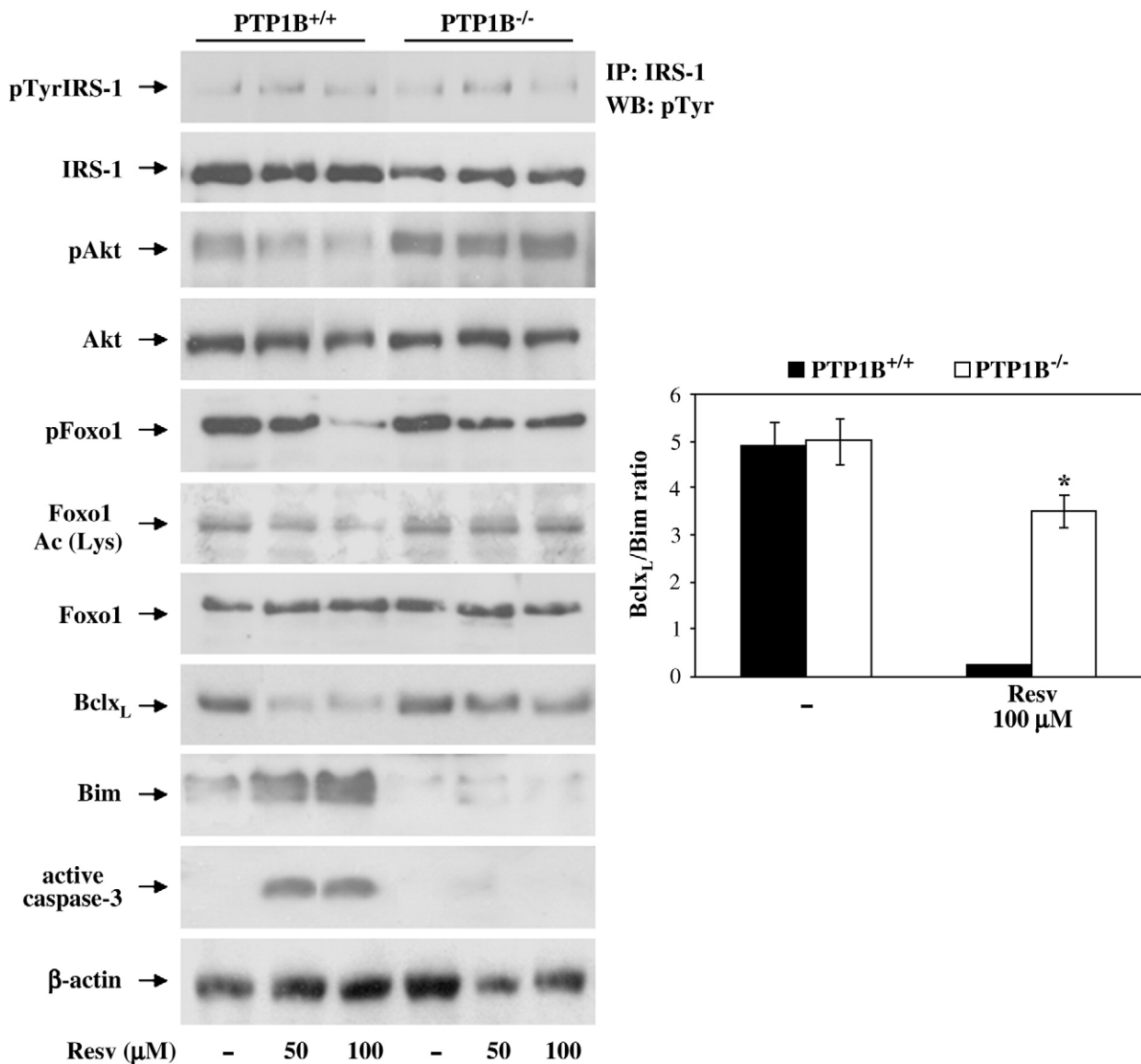


Fig. 7. Resveratrol decreases Akt phosphorylation and Foxo1 phosphorylation/deacetylation in wild-type, but not in PTP1B-deficient differentiated brown adipocytes. Differentiated PTP1B^{+/+} and PTP1B^{-/-} brown adipocytes were stimulated with resveratrol (50 or 100 μM) for 16 h. At the end of the culture time cells were lysed and 600 μg of total protein were immunoprecipitated with anti-IRS-1 antibody, and analyzed by Western blot with anti-pTyr antibody. Total protein was analyzed by Western blot with antibodies against IRS-1, phospho-Akt (ser-473), Akt, phospho-Foxo1 (ser-256), (Ac) Lys Foxo1, Foxo1, Bim, Bclx_L, active caspase-3, and β-actin. Representative images are shown. The autoradiograms corresponding to three independent experiments were quantitated by scanning densitometry and the Bclx_L/Bim ratio was calculated. * $p < 0.05$, PTP1B^{-/-} versus PTP1B^{+/+}.

controls. Finally, PTP1B^{-/-} brown adipocytes were resistant to the activation of the executor caspase-3 by resveratrol.

3.7. Re-expression of PTP1B in deficient brown preadipocytes delays differentiation and restores apoptotic sensitivity

Finally, to further demonstrate that PTP1B expression regulates the susceptibility to apoptotic triggers during differentiation and in fully differentiated brown adipocytes, we reconstituted PTP1B expression in PTP1B^{-/-} brown preadipocytes. The recovery of PTP1B expression in different cell lines (PTP1B^{-/-rec}) is depicted in Fig. 9A. For further experiments, we selected cell lines that expressed similar PTP1B levels as wild-type cells (clones 1, 5, and 6). As a control, we infected PTP1B^{-/-} cells with empty vector (PTP1B^{-/-hgy}). Both PTP1B^{-/-rec} and PTP1B^{-/-hgy} brown preadipocytes were submitted to the differentiation protocol and the expression of FAS and UCP1, key markers of adipogenic and thermogenic differentiation, respectively, was analyzed at day 6. As shown in Fig. 9B, both FAS and UCP1 levels were reduced in PTP1B^{-/-rec}

differentiated brown adipocytes as compared to PTP1B^{-/-hgy} controls. Moreover, the intensity of Oil Red O staining was also decreased after reconstitution of PTP1B expression. Next, we studied the effects of PTP1B rescue on the susceptibility to undergo apoptosis during the induction phase of brown adipocyte differentiation (0–48 h). The percentage of hypodiploid cells 48 h post-induction was threefold higher in PTP1B^{-/-rec} cells as compared to the PTP1B^{-/-hgy} controls (Fig. 9C), indicating that PTP1B re-expression restored the apoptotic rate during the induction phase. Of note, caspase-3 activity was significantly enhanced in PTP1B^{-/-rec} differentiating brown adipocytes at 24–48 h post-induction. Moreover, fully differentiated PTP1B^{-/-rec} brown adipocytes treated with TNFα plus CHX for 5 h showed a similar percentage of hypodiploid cells as wild-type brown adipocytes ($10.80 \pm 2.80\%$ in T + CHX-treated PTP1B^{-/-rec} cells versus $1.92 \pm 0.60\%$ in PTP1B^{-/-rec} untreated cells, see Fig. 4B). Similarly, resveratrol treatment for 16 h augmented the percentage of PTP1B^{-/-rec} hypodiploid cells ($12.90 \pm 2.3\%$ in resveratrol-treated PTP1B^{-/-rec} cells versus $1.80 \pm 0.76\%$ in PTP1B^{-/-rec} untreated cells).

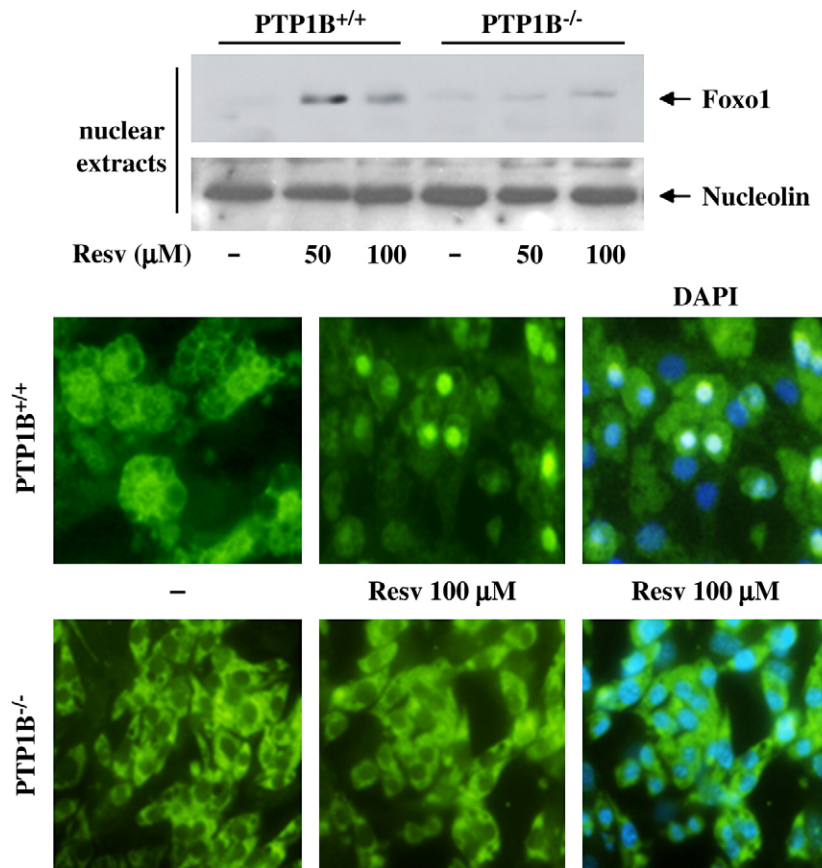


Fig. 8. PTP1B deficiency protects from resveratrol-induced Foxo1 nuclear accumulation. (upper panel) Nuclear protein (50 µg) was submitted to Western blot analysis with the anti-Foxo1 antibody. Nucleolin was used as a loading control. A representative experiment is shown. (lower panel) Immunofluorescence of Foxo1 in control and brown adipocytes treated with 100 µM resveratrol for 16 h. Representative images are shown.

3.8. Re-expression of PTP1B in deficient brown adipocytes decreases survival signalling pathways upon apoptotic stimulation

We finally explored the effects of PTP1B rescue on pro- and anti-apoptotic signalling upon TNF α plus CHX or resveratrol treatment. Differentiated PTP1B $^{-/-}$ rec or PTP1B $^{-/-}$ hyg brown adipocytes were stimulated with TNF α plus CHX for 5 h and IRS-1/Akt/PKB signalling was analyzed. As shown in Fig. 10A, IRS-1 tyrosine phosphorylation which remained elevated in TNF α plus CHX-treated PTP1B $^{-/-}$ hyg brown adipocytes, was substantially decreased in rescued cells in parallel to its degradation. Phosphorylation of Akt/PKB also decreased in PTP1B $^{-/-}$ rec brown adipocytes as compared to PTP1B $^{-/-}$ hyg cells. Regarding apoptotic signalling, TNF R oligomerization led to FLIP degradation, Bid cleavage, Bcl x_L down-regulation and activation of the executor caspase-3 only in PTP1B $^{-/-}$ rec cells. We next analyzed at the molecular level the response of both cell types to resveratrol. As shown in Fig. 10B, the recovery of PTP1B expression decreased Akt/PKB and Foxo1 phosphorylation in resveratrol-treated PTP1B $^{-/-}$ rec cells, as well as the acetylated state and the nuclear localization of the latter (see also Fig. 11). As a result, Bim expression was increased whereas Bcl x_L decreased similarly as in wild-type cells (Fig. 7). Therefore, resveratrol treatment triggered caspase-3 cleavage only in PTP1B $^{-/-}$ rec brown adipocytes.

4. Discussion

Adipocyte differentiation is a complex process that requires communication between extracellular stimuli in a coordinated network of receptors, signalling pathways and transcription factors. While most studies of adipogenesis have focused on the development

of WAT, less is known about brown fat adipogenesis. Insulin is a potent inducer of adipogenesis, and differentiation of brown adipocytes requires many components of the insulin signalling pathway. Among the critical nodes of insulin signalling, recent studies have revealed the specificity of IRA and IRB isoforms, as well as IRS proteins for brown adipocyte differentiation [23,41]. In the present report, using SV40 LT-antigen-immortalized brown preadipocytes isolated from wild-type and PTP1B $^{-/-}$ mice, we found that the percentage of cells accumulating fat droplets during differentiation was significantly increased in the absence of this phosphatase in comparison with PTP1B expressing cells. Consistent with the diminished number of fat-accumulating cells, the expression of transcription factors and coactivators that control adipocyte differentiation was more sustained along the time-course of differentiation in PTP1B-deficient brown adipocytes. Other features of brown adipocyte differentiation such as UCP-1, FAS, IRS-3 and caveolin-1 expression [39] and the presence of the IRB isoform [41] also indicated accelerated differentiation together with a better brown fat phenotype observed in the absence of PTP1B. It is noteworthy that the effect of PTP1B deficiency on brown adipocyte differentiation is opposite to that of the lack of IRS-1 [20]. As previously shown, IRS-1 is critical for the activation of the PI 3-kinase/Akt/PKB pathway in brown adipocytes [38]. On the other hand, our results clearly show that differentiated brown adipocytes lacking PTP1B exhibited insulin hypersensitivity. Thus, the absence of signals that positively or negatively regulate the insulin cascade trigger defects or improvements in brown adipocyte differentiation, respectively. In light of these results, we found improved responses to insulin in human hepatic cells pre-treated with conditioned medium from differentiating PTP1B $^{-/-}$ brown adipocytes which expressed higher adiponectin levels than the wild-type controls. Since it has been

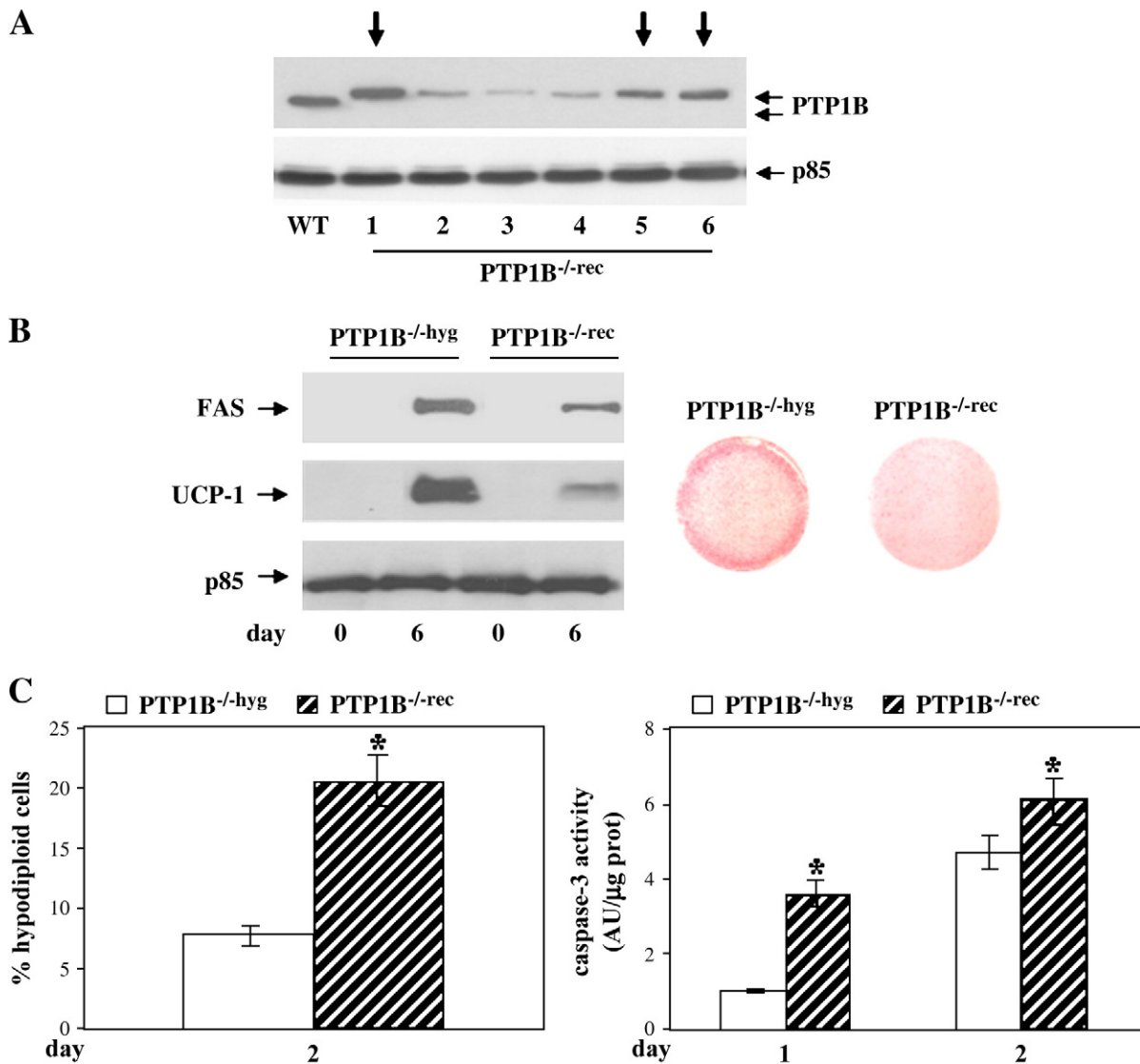


Fig. 9. Re-expression of PTP1B in PTP1B^{-/-} brown preadipocytes delays differentiation and restores the apoptotic sensitivity during the induction phase of differentiation. A. Immortalized PTP1B-deficient brown preadipocytes were reconstituted with retroviral PTP1B as described in Materials and Methods. PTP1B expression in different cell lines was assessed by Western blot. P85α-PI 3-kinase was used as a loading control. B. Reconstituted (PTP1B^{-/-}-rec) or PTP1B^{-/-} brown preadipocytes infected with empty retroviral vector (PTP1B^{-/-}-hyg) were submitted to the differentiation protocol. At day 6 of differentiation, cells were fixed and stained with Oil Red O or alternatively total protein lysates were prepared and the expression of UCP1 and FAS was analyzed by Western blot. p85α-PI 3-kinase was used as a loading control. A representative experiment is shown. Similar results were obtained with 3 different reconstituted cell lines C. (left panel) Reconstituted (PTP1B^{-/-}-rec) or PTP1B^{-/-}-hyg brown preadipocytes infected with empty retroviral vector were submitted to the differentiation protocol and the percentage of cells with DNA lower than 2C (apoptotic cells) was determined by flow cytometry after 48 h. Results are expressed as percentage of apoptotic cells are means \pm SE from three independent experiments. *p < 0.05, PTP1B^{-/-}-rec versus PTP1B^{-/-}-hyg. (right panel) Caspase-3 enzyme activity was measured in differentiating PTP1B^{-/-}-rec and PTP1B^{-/-}-hyg brown preadipocytes at 24 and 48 h. Results are expressed as arbitrary units/ μ g protein and are means \pm SE from three independent experiments. *p < 0.05, PTP1B^{-/-}-rec versus PTP1B^{-/-}-hyg.

reported that BAT expresses this adipokine [40], our data suggest that a possible mechanism for the enhancement of insulin signalling in brown adipocytes lacking PTP1B might be related to a positive cross-talk between insulin and adiponectin signalling.

When post-confluent, growth-arrested brown adipocyte precursor cells from wild-type mice were induced to differentiate into adipocytes apoptosis occurred within 24–48 h. Conversely, PTP1B^{-/-} brown preadipocytes were protected against apoptosis during this induction phase. Of note, the imbalance between pro- and anti-apoptotic members of the Bcl-2 family of proteins during the induction of differentiation was more severe in wild-type brown fat cells than in those lacking PTP1B. In addition, Akt/PKB phosphorylation, a major survival signal in mammalian cells, decreased more rapidly in differentiating brown preadipocytes expressing PTP1B. In the absence of Akt/PKB signalling, Foxo1 localizes predominantly to

the nucleus where it binds to promoters of target genes that induce cell death, such as FasL [51], Bim [45,46], and Bcl-6, a transcriptional repressor of Bclx_L [50]. Indeed, over-expression of Foxo1 or Foxo3a induces apoptosis in various cell types including immortalized hepatocytes [52–54]. Interestingly, PTP1B triggers substantial changes in the subcellular localization of Foxo1 in differentiating cells. The fact that nuclear localization of Foxo1 was only observed in wild-type cells 24 h after induction reflects actions of PTP1B upstream of Foxo1 nuclear translocation. This hypothesis strengthens the importance of the Akt/Foxo1 signalling pathway in the protection against apoptosis triggered by induction of differentiation in brown adipocytes. Among Foxo1 targets, the expression of FasL paralleled its nuclear localization with a significant delay in the absence of PTP1B. This effect, together with the constitutive down-regulation of Bid expression in PTP1B^{-/-} cells might explain the attenuation of caspase-8 activation during

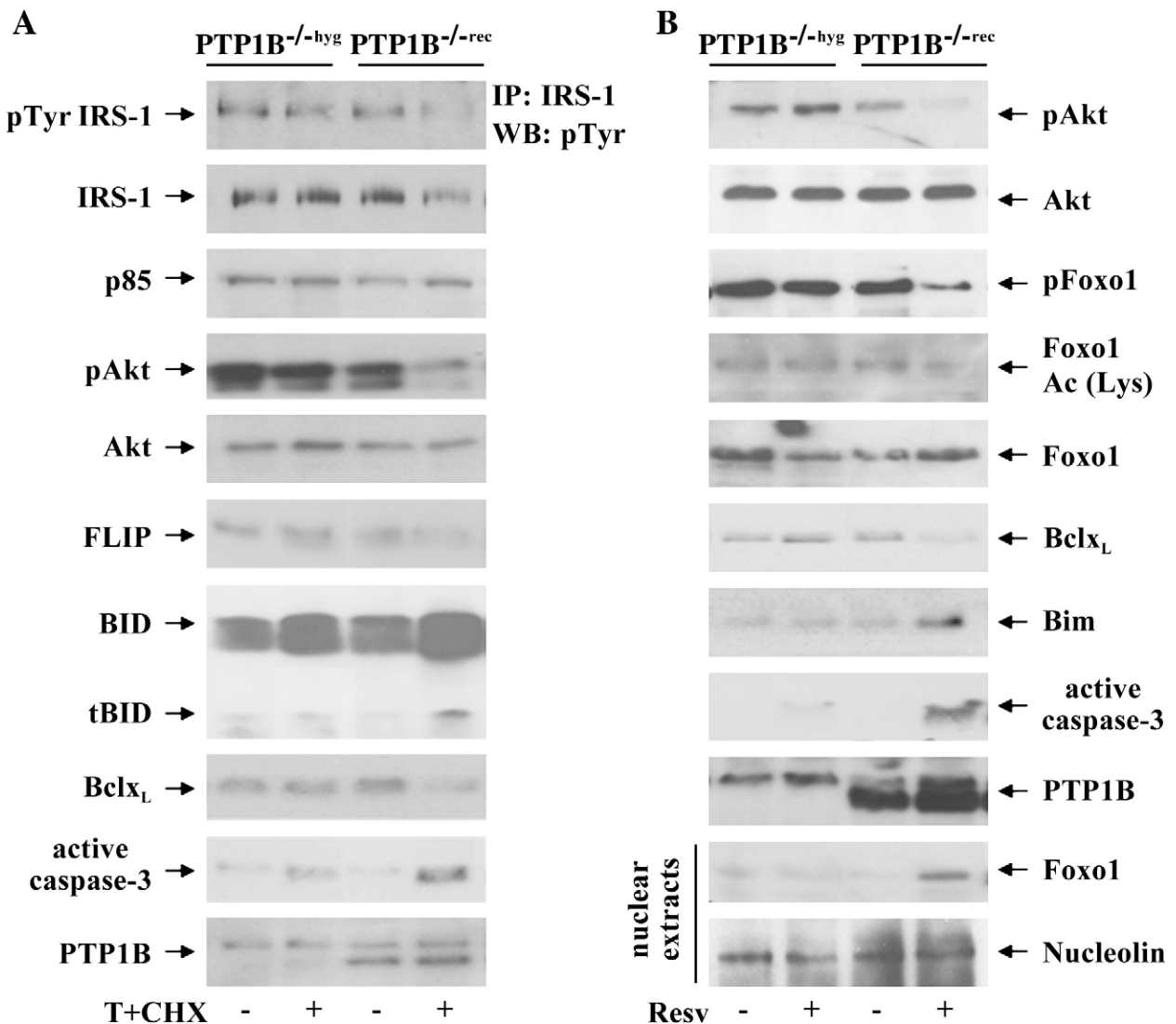


Fig. 10. Re-expression of PTP1B suppresses survival signalling and restores apoptotic pathways in brown adipocytes upon TNF α plus CHX or resveratrol treatment. A. Differentiated (day 6) PTP1B^{-/-}rec or PTP1B^{-/-}hyg brown adipocytes were treated with TNF α plus CHX (T + CHX) for 5 h or left untreated. At the end of the culture time cells were lysed and 600 μ g of total protein were immunoprecipitated with anti-IRS-1 antibody, and analyzed by Western blot with anti-pTyr antibody. Whole cell lysates were analyzed by Western blot with antibodies against IRS-1, phospho-Akt (ser-473), Akt, p85 α -PI 3 kinase, FLIP, Bid, Bclx_L, active caspase-3, and PTP1B. Representative autoradiograms are shown. B. (upper panel) Differentiated (day 6) PTP1B^{-/-}rec or PTP1B^{-/-}hyg brown adipocytes were treated with resveratrol (100 μ M) for 16 h or left untreated. At the end of the culture time, cells were lysed and whole cell lysates were analyzed by Western blot with antibodies against phospho-Akt (ser-473), Akt, phospho-Foxo1(ser-256), (Ac) Lys Foxo1, Foxo1, Bim, Bclx_L, active caspase-3 and PTP1B. Representative autoradiograms are shown. (lower panel) Nuclear protein (50 μ g) was submitted to Western blot analysis with the anti-Foxo1 antibody. Nucleolin was used as a loading control. A representative experiment is shown.

the induction phase. However, the expression of other Foxo1 targets such as Bim was not modulated by PTP1B, indicating that during differentiation this BH3-only protein is regulated by Foxo1-independent mechanisms.

Obesity has been associated with brown fat atrophy that leads to decreased energy expenditure. TNF α is highly expressed in adipose tissues of obese animals and humans [34,35]. This pro-inflammatory cytokine has also been shown to induce brown adipocyte apoptosis in

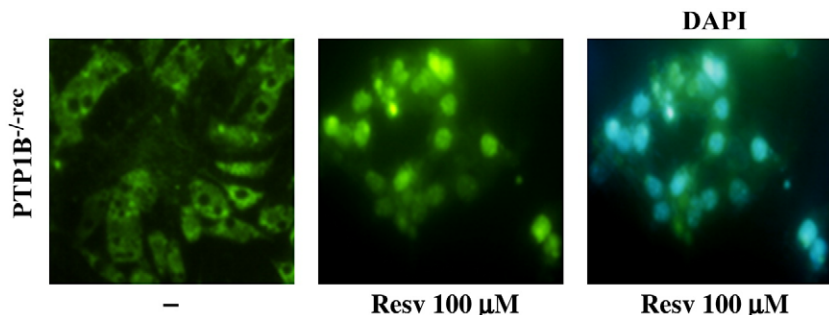


Fig. 11. Re-expression of PTP1B restores Foxo1 nuclear localization in resveratrol-treated brown adipocytes. Immunofluorescence of Foxo1 in PTP1B^{-/-}rec brown adipocytes treated with 100 μ M resveratrol for 16 h. Representative images are shown.

vitro [32,33]. Obese mice lacking either TNF α or its receptors showed protection against developing insulin resistance [55,56] and brown adipocyte apoptosis [57]. Our results show for the first time that PTP1B deficiency protects brown adipocytes against apoptosis triggered by TNF α . At the molecular level this protection was elicited at the DISC, an early event in the death-receptor apoptotic pathway. Thus, the subsequent molecular events of the apoptotic program that lead to the activation of the executor caspase-3 were totally abolished in brown adipocytes lacking PTP1B and rescued by re-expression of this phosphatase. In light of these results, it has been reported that PI 3-kinase/Akt/PKB activated by HGF-R coupling ensures high levels of FLIP, a critical step in the protection against its degradation by Fas in murine hepatocytes [58]. Interestingly, TNF α plus CHX treatment decreased Akt/PKB phosphorylation and FLIP levels in wild-type brown adipocytes, but not in those lacking PTP1B. In addition, in PTP1B $^{-/-}$ brown adipocytes protection against death receptor-mediated apoptosis correlated with the maintenance of high levels of the anti-apoptotic protein Bcl x_L compared to wild-type cells. These data are in agreement with our previous findings in PTP1B-deficient hepatocytes, showing a positive correlation between Akt/PKB phosphorylation, Bcl x_L levels, and cell survival [31]. Accordingly, the maintenance of high levels of FLIP and Bcl x_L during treatment with TNF α protects against apoptosis in differentiated PTP1B $^{-/-}$ brown adipose cells.

We have previously shown that in brown adipocytes activation of Akt/PKB is mediated by IRS-1 [38] which is a PTP1B substrate [25]. Moreover, it is well known that ser-307 phosphorylation triggers IRS-1 degradation via the proteasome, thereby switching off insulin signalling [59]. Thus, the lack of PTP1B in TNF α plus CHX-stimulated brown adipocytes maintained IRS-1 highly phosphorylated on tyrosine in spite of the transient ser-307 phosphorylation, resulting in the maintenance of normal tyrosine phosphorylation and protein levels. Since inhibition of PTP1B is at present being considered as a pharmacological approach to treat obesity and type 2 diabetes, our results strongly suggest that one potential benefit of PTP1B inhibitors might be the protection against brown fat atrophy provoked by elevated TNF α . In humans PTP1B inhibition could be therapeutically relevant, since brown fat depots are localized within white fat [5,60].

Besides TNF α , little is known about additional stimuli that trigger brown adipocyte cell death. Very recently attention has focused on natural phytochemicals due to their potential benefits for reducing the incidence of cancer and metabolic syndrome. Among them, resveratrol has been shown to decrease proliferation and induce apoptosis and cell cycle arrest in various cell lines, including 3 T3-L1 adipocytes [37]. When we investigated the impact of PTP1B deficiency in brown adipocytes on the susceptibility to undergo apoptosis triggered by resveratrol, we found opposite responses, depending on the expression of this phosphatase. Whereas resveratrol induced a marked increase in the percentage of apoptotic wild-type brown adipocytes, PTP1B-deficient cells were refractory to resveratrol-induced cell death. At the molecular level, resveratrol failed to activate the death receptor pathway (data not shown). Besides, resveratrol treatment maintained an increased Bcl x_L /Bim ratio in PTP1B $^{-/-}$ brown adipocytes as compared to the wild-type controls. These results clearly indicate that PTP1B levels modulate the balance between the expression of these anti-apoptotic (Bcl x_L) and pro-apoptotic (Bim) Bcl-2 family proteins in response to resveratrol, which may influence the subsequent cellular events of the intrinsic apoptotic pathway leading to executor caspase-3 activation and cell death.

Recently it has been shown that activation of Sirt1 by resveratrol deacetylates Foxo1 and renders it immobile within the nuclear compartment, thereby promoting Foxo1-dependent transcription [49]. Our results show that in wild-type brown adipocytes resveratrol treatment leads to Akt/PKB and Foxo1 dephosphorylation/deacetylation in parallel with Foxo1 nuclear accumulation. By contrast, in resveratrol-treated PTP1B $^{-/-}$ brown adipocytes phosphorylation of

Akt/PKB and phosphorylation/acetylation of Foxo1 remained elevated, and hence Foxo1 did not translocate to the nucleus. Although IRS-1 is a common upstream mediator of Akt/PKB activation, IRS-1 degradation nor decreased tyrosine phosphorylation were observed upon resveratrol treatment in either kind of brown adipocyte. Thus, IRS-1-independent signalling might be involved in the disruption of Akt/PKB activation by promoting its dephosphorylation. Another possibility to explain these results could be the inactivation of the Akt/PKB ser-473 phosphatase PP2A by tyrosine dephosphorylation in the absence of PTP1B. However, PP2A tyrosine phosphorylation was unaffected by PTP1B deficiency or resveratrol treatment (data not shown). Thus, additional negative signals triggering the inactivation of Akt/PKB by resveratrol in brown adipocytes need to be further investigated.

In conclusion, our results show for the first time that PTP1B inhibition protects against apoptosis during the induction phase of differentiation through the maintenance of intact Akt/PKB survival signalling and high Bcl x_L levels. This molecular mechanism could also be responsible for the protection against TNF α - or resveratrol-mediated apoptosis in differentiated brown adipocytes in an IRS-1-dependent and independent manner, respectively. Due to the contribution of brown fat to energy homeostasis, inhibition of PTP1B could avoid TNF α -induced brown fat atrophy in therapies against obesity and in combination with resveratrol might improve low-grade inflammation.

Acknowledgements

This work was supported by grants SAF2009-08114 and CITE-090100-2007-35 (MCINN, Spain), and by the Centro de Investigación Biomédica en Red de Diabetes y Enfermedades Metabólicas Asociadas (CIBERDEM), Instituto Carlos III, MCINN, (Spain). We thankfully acknowledge Paloma Martín-Sanz (CSIC, Spain) for supplying CHL human liver cells.

References

- [1] D.G. Nicholls, R.M. Locke, *Physiol. Rev.* 64 (1) (1984) 1.
- [2] P. Trayhurn, R.E. Milner, *Can. J. Physiol. Pharmacol.* 67 (8) (1989) 811.
- [3] D. Ricquier, "F" Bouillaud, *Biochem. J.* 345 (Pt 2) (2000) 161.
- [4] P. Trayhurn, in: PT, DG N (Eds.), *Brown adipose tissue*, Edward Arnold Ltd, London, 1986, p. 299.
- [5] A.M. Cypress, S. Lehman, G. Williams, I. Tal, D. Rodman, A.B. Goldfine, F.C. Kuo, E.L. Palmer, Y.H. Tseng, A. Doria, G.M. Kolodny, "CR" Kahn, *N. Engl. J. Med.* 360 (15) (2009) 1509.
- [6] M. Lorenzo, A.M. Valverde, T. Teruel, "M" Benito, *J. Cell Biol.* 123 (6 Pt 1) (1993) 1567.
- [7] T. Teruel, A.M. Valverde, A. Alvarez, M. Benito, M. Lorenzo, *Biochem. J.* 310 (Pt 3) (1995) 771.
- [8] T. Teruel, A.M. Valverde, M. Benito, M. Lorenzo, *Biochem. J.* 319 (Pt 2) (1996) 627.
- [9] G. Ailhaud, P. Grimaldi, R. Negrel, *Annu. Rev. Nutr.* 12 (1992) 207.
- [10] P. Puigserver, J. Ribot, F. Serra, M. Giannotti, M.L. Bonet, B. Nadal-Ginard, A. Palou, *Eur. J. Cell Biol.* 77 (2) (1998) 117.
- [11] P. Yubero, C. Manchado, A.M. Cassard-Doulcier, T. Mampel, O. Vinas, R. Iglesias, M. Giralt, F. Villarroya, *Biochem. Biophys. Res. Commun.* 198 (2) (1994) 653.
- [12] I.B. Sears, M.A. MacGinnitie, L.G. Kovacs, R.A. Graves, *Mol. Cell. Biol.* 16 (7) (1996) 3410.
- [13] P. Puigserver, Z. Wu, C.W. Park, R. Graves, M. Wright, B.M. Spiegelman, *Cell* 92 (6) (1998) 829.
- [14] Z. Wu, P. Puigserver, U. Andersson, C. Zhang, G. Adelman, V. Mootha, A. Troy, S. Cinti, B. Lowell, R.C. Scarpulla, B.M. Spiegelman, *Cell* 98 (1) (1999) 115.
- [15] A.M. Valverde, M. Arribas, C. Mur, P. Navarro, S. Pons, A.M. Cassard-Doulcier, C.R. Kahn, M. Benito, *J. Biol. Chem.* 278 (12) (2003) 10221.
- [16] M.I. Lefterova, Y. Zhang, D.J. Steger, M. Schupp, J. Schug, A. Cristancho, D. Feng, D. Zhuo, C.J. Stoeckert Jr., X.S. Liu, M.A. Lazar, *Genes Dev.* 22 (21) (2008) 2941.
- [17] R. Nielsen, T.A. Pedersen, D. Hagenbeek, P. Moulos, R. Siersbaek, E. Megens, S. Denissov, M. Borgesen, K.J. Francojs, S. Mandrup, H.G. Stunnenberg, *Genes Dev.* 22 (21) (2008) 2953.
- [18] Z. Wu, E.D. Rosen, R. Brun, S. Hauser, G. Adelman, A.E. Troy, C. McKeon, G.J. Darlington, B.M. Spiegelman, *Mol. Cell.* 3 (2) (1999) 151.
- [19] Y.H. Tseng, E. Kokkotou, T.J. Schulz, T.L. Huang, J.N. Winnay, C.M. Taniguchi, T.T. Tran, R. Suzuki, D.O. Espinoza, Y. Yamamoto, M.J. Ahrens, A.T. Dudley, A.W. Norris, R.N. Kulkarni, C.R. Kahn, *Nature* 454 (7207) (2008) 1000.
- [20] M. Fasshauer, J. Klein, K.M. Kriauciunas, K. Ueki, M. Benito, C.R. Kahn, *Mol. Cell. Biol.* 21 (1) (2001) 319.
- [21] M. Arribas, A.M. Valverde, D. Burks, J. Klein, R.V. Farese, M.F. White, M. Benito, *FEBS Lett.* 536 (1–3) (2003) 161.

- [22] M. Fasshauer, J. Klein, K. Ueki, K.M. Kriauciunas, M. Benito, M.F. White, C.R. Kahn, *J. Biol. Chem.* 275 (33) (2000) 25494.
- [23] Y.H. Tseng, K.M. Kriauciunas, E. Kokkotou, C.R. Kahn, *Mol. Cell. Biol.* 24 (5) (2004) 1918.
- [24] M. Arribas, A.M. Valverde, M. Benito, *J. Biol. Chem.* 278 (46) (2003) 45189.
- [25] B.J. Goldstein, A. Bittner-Kowalczyk, M.F. White, M. Harbeck, *J. Biol. Chem.* 275 (6) (2000) 4283.
- [26] B.L. Seely, P.A. Staubs, D.R. Reichart, P. Berhanu, K.L. Milar斯基, A.R. Saltiel, J. Kusari, J. M. Olefsky, *Diabetes* 45 (10) (1996) 1379.
- [27] M. Elchebly, P. Payette, E. Michaliszyn, W. Cromlish, S. Collins, A.L. Loy, D. Normandin, A. Cheng, J. Himms-Hagen, C.C. Chan, C. Ramachandran, M.J. Gresser, M.L. Tremblay, B.P. Kennedy, *Science* 283 (5407) (1999) 1544.
- [28] L.D. Klaman, O. Boss, O.D. Peroni, J.K. Kim, J.L. Martino, J.M. Zabolotny, N. Moghal, M. Lubkin, Y.B. Kim, A.H. Sharpe, A. Stricker-Krongrad, G.I. Shulman, B.G. Neel, B.B. Kahn, *Mol. Cell. Biol.* 20 (15) (2000) 5479.
- [29] N. Dube, M.L. Tremblay, *Biochim. Biophys. Acta* 1754 (1–2) (2005) 108.
- [30] V. Sangwan, G.N. Paliouras, A. Cheng, N. Dube, M.L. Tremblay, M. Park, *J. Biol. Chem.* 281 (1) (2006) 221.
- [31] A. Gonzalez-Rodriguez, O. Escribano, J. Alba, C.M. Rondinone, M. Benito, A.M. Valverde, *J. Cell. Physiol.* 212 (1) (2007) 76.
- [32] E. Nisoli, A. Cardile, A. Bulbarelli, L. Tedesco, R. Bracale, V. Cozzi, M. Morroni, S. Cinti, A. Valerio, M.O. Carruba, *Cell Death Differ.* 13 (12) (2006) 2154.
- [33] A. Porras, A.M. Alvarez, A. Valladares, M. Benito, *FEBS Lett.* 416 (3) (1997) 324.
- [34] G.S. Hotamisligil, N.S. Shargill, B.M. Spiegelman, *Science* 259 (5091) (1993) 87.
- [35] G.S. Hotamisligil, P. Arner, J.F. Caro, R.L. Atkinson, B.M. Spiegelman, *J. Clin. Invest.* 95 (5) (1995) 2409.
- [36] H.J. Park, J.Y. Yang, S. Ambati, M.A. Della-Fera, D.B. Hausman, S. Rayalam, C.A. Baile, *J. Med. Food* 11 (4) (2008) 773.
- [37] J.Y. Yang, M.A. Della-Fera, S. Rayalam, S. Ambati, D.L. Hartzell, H.J. Park, C.A. Baile, *Life Sci.* 82 (19–20) (2008) 1032.
- [38] A.M. Valverde, C.R. Kahn, xM. Benito, *Diabetes* 48 (11) (1999) 2122.
- [39] O. Escribano, M. Arribas, A.M. Valverde, M. Benito, *Mol. Cell. Endocrinol.* 268 (1–2) (2007) 1.
- [40] N. Fujimoto, N. Matsuo, H. Sumiyoshi, K. Yamaguchi, T. Saikawa, H. Yoshimatsu, H. Yoshioka, *Biochim. Biophys. Acta* 1731 (1) (2005) 1.
- [41] A.J. Entingh, C.M. Taniguchi, C.R. Kahn, *J. Biol. Chem.* 278 (35) (2003) 33377.
- [42] O.A. MacDougald, M.D. Lane, *Curr. Biol.* 5 (6) (1995) 618.
- [43] A. Parcellier, L.A. Tintignac, E. Zhuravleva, B.A. Hemmings, *Cell. Signal.* 20 (1) (2008) 21.
- [44] J. Nakae, V. Barr, D. Accili, *Embo J.* 19 (5) (2000) 989.
- [45] P.F. Dijkers, R.H. Medema, J.W. Lammers, L. Koenderman, P.J. Coffer, *Curr. Biol.* 10 (19) (2000) 1201.
- [46] M. Stahl, P.F. Dijkers, G.J. Kops, S.M. Lens, P.J. Coffer, B.M. Burgering, R.H. Medema, *J. Immunol.* 168 (10) (2002) 5024.
- [47] K. Ishizuka, I. Usui, Y. Kanatani, A. Bukhari, J. He, S. Fujisaka, Y. Yamazaki, H. Suzuki, K. Hiratani, M. Ishiki, M. Iwata, M. Urakaze, T. Haruta, M. Kobayashi, *Endocrinology* 148 (6) (2007) 2994.
- [48] J. Zhu, W. Yong, X. Wu, Y. Yu, J. Lv, C. Liu, X. Mao, Y. Zhu, K. Xu, X. Han, C. Liu, *Biochem. Biophys. Res. Commun.* 369 (2) (2008) 471.
- [49] D. Frescas, L. Valenti, D. Accili, *J. Biol. Chem.* 280 (21) (2005) 20589.
- [50] T.T. Tang, D. Dowbenko, A. Jackson, L. Toney, D.A. Lewin, A.L. Dent, L.A. Lasky, *J. Biol. Chem.* 277 (16) (2002) 14255.
- [51] T. Suhara, H.S. Kim, L.A. Kirshenbaum, K. Walsh, *Mol. Cell. Biol.* 22 (2) (2002) 680.
- [52] A. Brunet, A. Bonni, M.J. Zigmond, M.Z. Lin, P. Juo, L.S. Hu, M.J. Anderson, K.C. Arden, J. Blenis, M.E. Greenberg, *Cell* 96 (6) (1999) 857.
- [53] E.D. Tang, G. Nunez, F.G. Barr, K.L. Guan, *J. Biol. Chem.* 274 (24) (1999) 16741.
- [54] A.M. Valverde, I. Fabregat, D.J. Burks, M.F. White, M. Benito, *Hepatology* 40 (6) (2004) 1285.
- [55] K.T. Uysal, S.M. Wiesbrock, G.S. Hotamisligil, *Endocrinology* 139 (12) (1998) 4832.
- [56] K.T. Uysal, S.M. Wiesbrock, M.W. Marino, G.S. Hotamisligil, *Nature* 389 (6651) (1997) 610.
- [57] E. Nisoli, L. Briscini, A. Giordano, C. Tonello, S.M. Wiesbrock, K.T. Uysal, S. Cinti, M. O. Carruba, G.S. Hotamisligil, *Proc. Natl. Acad. Sci. U. S. A.* 97 (14) (2000) 8033.
- [58] A. Moumen, A. Ieraci, S. Patane, C. Sole, J.X. Comella, R. Dono, F. Maina, *Hepatology* 45 (5) (2007) 1210.
- [59] R. Zhande, J.J. Mitchell, J. Wu, X.J. Sun, *Mol. Cell. Biol.* 22 (4) (2002) 1016.
- [60] M. Saito, Y. Okamatsu-Ogura, M. Matsushita, K. Watanabe, T. Yoneshiro, J. Nio-Kobayashi, T. Iwanaga, M. Miyagawa, T. Kameya, K. Nakada, Y. Kawai, M. Tsujisaki, *Diabetes* 58 (7) (2009) 1526.